BIOLOGY OF REPRODUCTION 71, 973–978 (2004)
Published online before print 19 May 2004.
DOI 10.1095/biolreprod.103.024422

Decrease of Fertilizing Ability of Mouse Spermatozoa after Freezing and Thawing Is Related to Cellular Injury[1]

Hirofumi Nishizono,[3,4] Masaki Shioda,[5] Toru Takeo,[6] Tetsumi Irie,[6] and Naomi Nakagata[2,4]

Kyudo Company Limited,[3] Kumamoto 861-0104, Japan
Center for Animal Resources and Development,[4] Kumamoto University, Kumamoto 860-0811, Japan
Department of Materials and Life Science,[5] Graduate School of Science and Technology, Kumamoto University, Kumamoto 860-8555, Japan
Department of Clinical Chemistry and Informatics,[6] Graduate School of Medical and Pharmaceutical Sciences, Kumamoto University, Kumamoto 860-8555, Japan

ABSTRACT

In general, the fertilizing ability of cryopreserved mouse spermatozoa is less than that of fresh spermatozoa. This ability is especially low in C57BL/6, the main strain used for the production of transgenic mice. To solve this problem, the relationship between cell damage and fertilizing ability in cryopreserved mouse spermatozoa was examined in this study. Sperm motility analysis revealed no significant difference among the motilities of cryopreserved C57BL/6J, BALB/cA, and DBA/2N sperm (67.6%, 43.4%, and 60.0%, respectively) after thawing. However, the results of in vitro fertilization (IVF), scanning electron microscopy (SEM), and transmission electron microscopy (TEM) showed a strong correlation between the frequency of aberrant spermatozoa (FAS) and fertilization rates (FR; C57BL/6J: FAS, 83.7%; FR, 17.0%; BALB/cA: FAS, 67.2%; FR, 24.2%; and DBA/2N: FAS, 10.2%; FR, 93.6%), and damage to spermatozoa was localized particularly in the acrosome of the head and mitochondria.

fertilization, in vitro fertilization, male reproductive tract, sperm, sperm motility and transport

INTRODUCTION

Over the past 15 years, a large number of transgenic and targeted mutant mice have been produced worldwide [1, 2]. In addition, N-ethyl-N-nitrosourea mutagenesis projects have been progressing, leading to an enormous increase in the number of strains of mutant mice that will be produced over the next few years [3, 4]. As a result, across the world animal facilities have an excess of mutant mice [5]. To solve this problem, sperm freezing may provide a much simpler and more economical alternative to embryo freezing [6–8].

In 1990, Yokoyama et al. [9] and Tada et al. [10] reported the successful freezing of mouse sperm using a solution containing glycerol and raffinose. Okuyama et al. [11] then found that mouse sperm can be frozen in a solution containing raffinose and skim milk without glycerol. We were also subsequently successful in the cryopreservation of mouse spermatozoa, including transgenic strains (luciferase transgenic mouse), using an improved method [12, 13]. These results indicated that slow dilution after thawing prevents the sharp change in osmolarity and viscosity between the cryopreservation solution and diluent. Moreover, Thornton et al. [14] have demonstrated that it is possible to establish efficient, comprehensive, and extensive archives, and that potentially large numbers of offspring (>7000) can be derived from the frozen spermatozoa of a single mutant male mouse.

However, in general, high fertilization rates are not always obtained for the frozen spermatozoa of all mouse strains [15]. Notably, the fertilization rate of frozen C57BL/6 spermatozoa remains very low, although the rate can be increased by in vitro fertilization with partial zona pellucida dissection or the intracytoplasmic sperm injection technique [16, 17]. C57BL/6 is a major inbred strain, and its genetic background is well known. Furthermore, this strain is used not only for the production of transgenic mice [18], but also as a backcross for targeted mutant mice. Therefore, it is necessary to establish a cryopreservation method for C57BL/6 mouse spermatozoa that can maintain high fertilizing ability after thawing. In this study, C57BL/6 frozen-thawed mouse spermatozoa were examined ultrastructurally for any damage that could account for their low fertilizing ability.

MATERIALS AND METHODS

Animals

Inbred male (12- to 20-week-old) and female (8- to 12-week-old) C57BL/6J, BALB/cA, and DBA/2N mice were purchased from CLEA Japan, Inc. (Tokyo, Japan). Homozygous transgenic male (12- to 20-week-old) mice expressing the enhanced green fluorescent protein (EGFP) gene under the acrosin promoter on C57BL/6J background, acr3-EGFP [19, 20], were provided from the mouse embryo bank of Mitsubishi Kagaku Institute of Life Sciences (Machida-shi, Tokyo, Japan). All mice were kept according to the Guidelines for Animal Experiments of Kumamoto University and the Guide for the Care and Use of Laboratory Animals. They were maintained on a constant 12D:12L cycle with standard mouse chow and water available ad libitum.

Sperm Freezing and Thawing

Spermatozoa were obtained from C57BL/6J, BALB/cA, DBA/2N, and acr3-EGFP male mice (5 males/strain). After the male mice were killed humanely, one caudae epididymis was removed and placed into an 18% raffinose/3% skim milk solution. Spermatozoa from other caudae epididymides were used as a noncryopreserved control (fresh). Sperm cryopreservation and thawing were performed as described previously [15]. Briefly, 0.25-ml plastic straws (IMV, Paris, France) with 10-μl sperm aliquots collected at room temperature were frozen by exposure to liquid nitrogen

[1]Supported by a Grant-in-Aid for Scientific Research, 11177101-04, from the Japan Society for the Promotion of Science.
[2]Correspondence: Naomi Nakagata, 2-2-1 Honjo, Kumamoto 860-0811, Japan. FAX: +81 96 373 6560; e-mail: nakagata@gpo.kumamoto-u.ac.jp

Received: 18 October 2003.
First decision: 28 October 2003.
Accepted: 14 May 2004.

ISSN: 0006-3363. http://www.biolreprod.org

vapor for 15 min before storage under liquid nitrogen. After 5 days, the samples were thawed in a water bath at 37°C for 10–15 min.

The thawed sperm suspension was incubated for 1.5 h with 5% CO_2 in air at 37°C in a 200-μl drop of human tubal fluid (HTF) medium [21] prepared in our laboratory and covered with paraffin oil (NACALAI TESQUE Inc., Kyoto, Japan). Thawed C57BL/6J sperm samples were evaluated using five experiments: in vitro fertilization (IVF), motility analysis, scanning electron microscopy (SEM), transmission electron microscopy (TEM), and zona-free assay. The DBA/2N sperm samples were evaluated using four experiments: IVF, motility analysis, SEM, and TEM. The BALB/cA sperm samples were evaluated using three experiments: IVF, motility analysis, and SEM. The acr3-EGFP sperm sample was evaluated using an acrosomal status assay.

In Vitro Fertilization

Inbred female mice were superovulated using an injection (i.p.) of 5 IU of eCG (Sigma Chemical Company, St. Louis, MO) followed by 5 IU of hCG (Sigma) 48 h later. Fourteen to fifteen h after the hCG injection, the females were killed and their oviducts were removed. The oocyte-cumulus complexes were isolated in a 200-μl drop of HTF medium covered with paraffin oil.

After the spermatozoa in the frozen plastic straw had thawed, the thawed sperm suspension was added to a 200-μl drop of HTF medium for IVF. The average concentration of these sperm was 8000 cells/μl. Five microliters of sperm suspension was added to the IVF medium (HTF) containing the oocyte-cumulus complexes (final sperm concentration = 200/μl). The IVF medium was placed in a sealed, modular incubator chamber gassed with 5% CO_2 in air and maintained at 37°C for 8 h. The oocytes were then washed to eliminate excess sperm and were mounted in toto on a slide stained with lacmoid (whole-mount staining). The whole-mount staining samples were examined to assess fertilization. When totals of fertilized egg and unfertilized egg were less than 80, the data were not accepted.

Motility Analysis

The concentrations and motility rates of the fresh control and the frozen-thawed samples were determined using a C-IMAGING C-MEN computerized semen analyzer (Compix Inc., Lake Oswego, OR). The average number of cells counted per sample was approximately 2000. All counts were performed at 37°C. Motility was defined as linear direction at a speed of 50 μm/sec [22].

Scanning Electron Microscopy

Mouse spermatozoa (fresh or frozen-thawed) were incubated in HTF for 20 min at 37°C, washed twice with HTF, and fixed in 2.5% glutaraldehyde (EM Sciences, Fort Washington, PA) for 4 h at 4°C. The sperm samples were washed with PBS (IATRON Laboratories Inc., Tokyo, Japan) and incubated overnight at 4°C. The samples were then fixed in 2% osmic acid (EM Sciences); dehydrated sequentially in 50%, 70%, 80%, 90%, 95%, and 100% ethanol; critical point-dried in a critical point dryer; coated with palladium gold; and examined with a scanning electron microscope (S-800, Hitachi High-Technologies Co., Tokyo, Japan). When fewer than 80 sperm were visible in a fixed sample, the data were not used.

In Vitro Fertilization Using Zona-Free Oocytes

The oocyte-cumulus complexes were obtained from the oviducts of superovulated C57BL/6J female mice. Cumulus cells were removed by incubating the complexes for 3 min in HTF medium containing 0.1% hyaluronidase (type IV; Sigma). After washing in fresh HTF medium, the zona pellucida was dissolved by treating the oocyte for 30 sec to 1 min with acid Tyrode solution (pH 2.5). Finally, zona-free oocytes were washed in HTF medium 3 times and were used for in vitro fertilization. To assess fertilization, the zona-free oocytes were examined using lacmoid staining.

Transmission Electron Microscopy

The fresh and frozen-thawed spermatozoa were prefixed in 2.5% glutaraldehyde/0.1 M phosphate buffer (PB, pH 7.4) for 2 h at 4°C and post-fixed in 2% osmium tetroxide in PB for 2 h at 4°C. This was followed by dehydration and embedding in Epon 812 (TAAB Laboratories Equipment Ltd., Aldermaston, England). To select the optimal areas for this study, semithin sections were stained with toluidine blue. Ultrathin sections stained with uranyl acetate and lead citrate were examined via TEM (JEM-1230; JEOL, Tokyo, Japan).

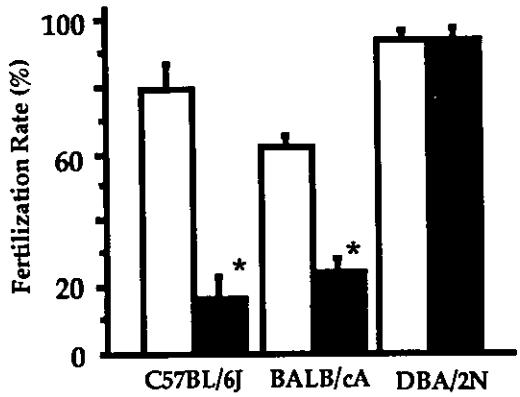

FIG. 1. The fertilization rate using fresh sperm (open bars) and frozen-thawed sperm (closed bars) from C57BL/6J, BALB/cA, and DBA/2N strains. Results are expressed as the mean ± SEM. $^*P < 0.05$, as compared with the fresh control.

Acrosomal Contents Status Assay Using acr3-EGFP Transgenic Mice

To assess the acrosomal contents, spermatozoa obtained from male acr3-EGFP transgenic mice were used. Immediately after collection from one caudae epididymis, the spermatozoa (fresh controls) were fixed for 5 min in 4% paraformaldehyde/PBS at room temperature [19]. Spermatozoa of other caudae epididymides were cryopreserved and then fixed after thawing (frozen-thawed samples). To determine whether acrosomal contents were present, samples (fresh and frozen-thawed) were observed under a fluorescent microscope.

Statistical Analyses

Normality of all variables was assessed through the use of the Kolmogorov-Smirnov test. Variables that were not normally distributed were arcsine transformed to approximate normality. Differences between in vitro fertilization rates before and after freezing were assessed with the paired *t*-test. The paired *t*-test was also used to analyze the difference in motility percentage of fresh and frozen sperm. The relation between fertility and the motility rate or cellular injury of spermatozoa was investigated by means of Pearson correlation coefficient. A significance level of 0.05 was used for all statistical tests, and two-tailed tests were applied. All statistical analyses were performed with Statview 5.0-J (SAS Institute Inc., Cary, NC).

RESULTS

In Vitro Fertilization Rate with Frozen Mouse Spermatozoa

The fertilizing rate using fresh control and frozen-thawed sperm from three strains is shown in Figure 1. The fertilizing ability of frozen C57BL/6J and BALB/cA spermatozoa was less than that of fresh spermatozoa. In DBA/2N mice, the fertilizing ability of fresh and frozen-thawed sperm was identical, whereas all other strains had a significantly reduced rate.

Sperm Motility after Freezing and Thawing

In order to elucidate the cause of decreased fertilizing ability in cryopreserved mouse spermatozoa, the sperm motility of frozen-thawed samples was examined. Figure 2 summarizes the motility of frozen-thawed sperm. Although the motility rates of frozen spermatozoa were lower than fresh spermatozoa, there was no significant difference

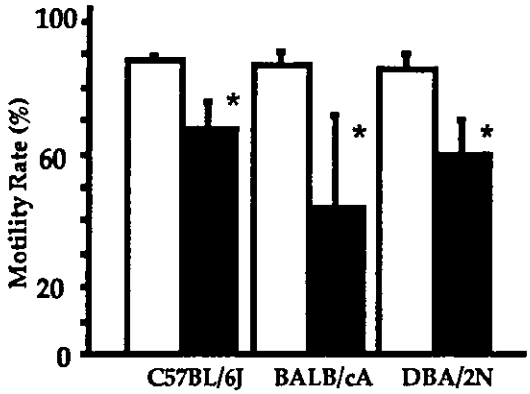

FIG. 2. Comparison of sperm motility using fresh sperm (open bars) and frozen-thawed sperm (closed bars) from three strains. Results are expressed as the mean ± SEM. $^*P < 0.05$, as compared with the fresh control.

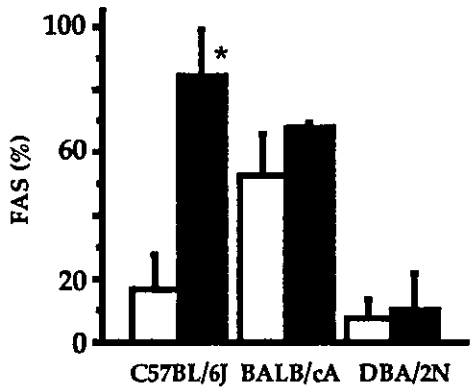

FIG. 4. Frequency of aberrant spermatozoa (FAS) in three strains. Fresh (open bars) and frozen-thawed spermatozoa (closed bars). Results are expressed as the mean ± SEM. $^*P < 0.05$, as compared with the fresh control.

among the motility rates of frozen spermatozoa in the three strains ($P > 0.05$).

Scanning Electron Microscopy

The cell surface of frozen-thawed mouse spermatozoa was studied morphologically (Fig. 3, A–F). Fresh sperm showed few abnormalities, whereas frozen/thawed sperm lacked the rostral tip of the head (Fig. 3B); had disrupted acrosomes (Fig. 3, B, E, and F, arrowheads); lacked part of the mitochondrial sheath (Fig. 3C, arrowhead); showed a swollen flagellar base (Fig. 3C, arrow); and had coiled flagella (Fig. 3D, arrowhead). In the DBA/2N strain, abnormal cells were observed, but at a low rate (Fig. 4, 10.2%). As shown in Figure 4, the ratio of abnormal cells in other strains was higher than in DBA/2N. Notably, in C57BL/6J, almost all the sperm had suffered cellular injury.

Cellular injury induced by freezing and thawing was mainly localized to the sperm head (81.2%). The middle piece and the tail of sperm were also damaged, although not severely. Furthermore, the dorsal anterior plasma membrane of the sperm head had notable defects, whereas the equatorial region and posterior head were normal after cryotreatment (Fig. 3, B, E, and F, arrowheads).

Transmission Electron Microscopy

To identify further causes of low fertility in frozen-thawed sperm, the ultrastructure was studied using TEM (Fig. 5, A–H). In the C57BL/6J strain, the plasma membrane changes in the acrosomal region were much more pronounced, whereas fresh sperm and DBA/2N spermatozoa did not show these defects (Fig. 5, A–D). Notably, both fresh controls and frozen DBA/2N spermatozoa had hydro-

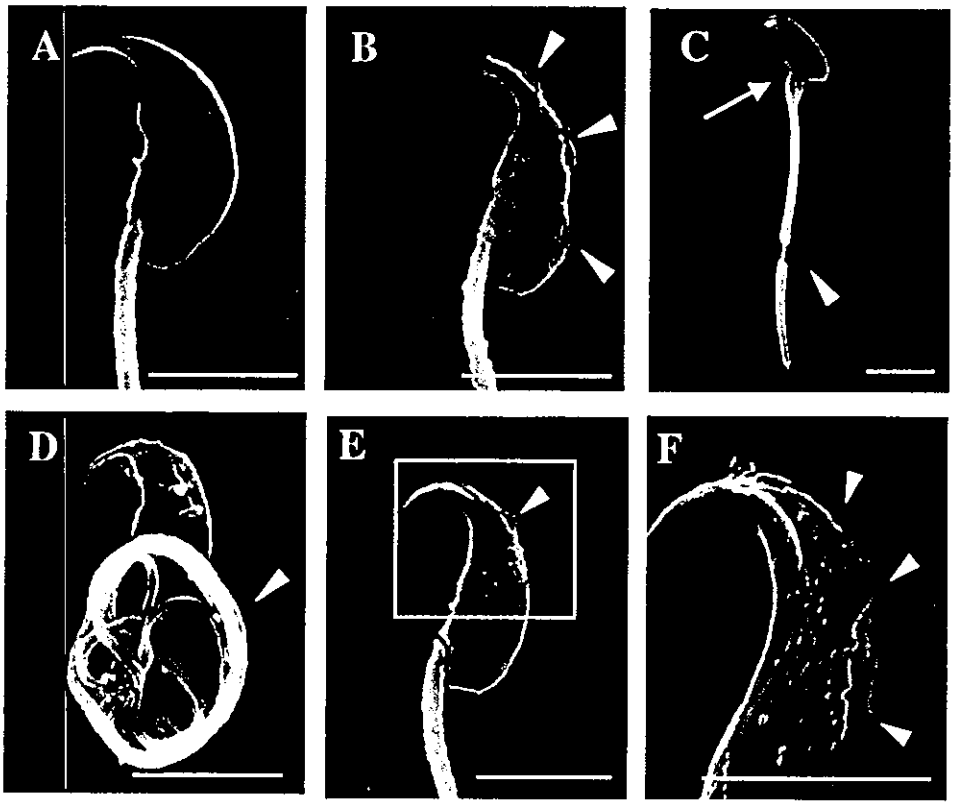

FIG. 3. Scanning electron micrographs of sperm from three strains. Fresh sperm (A) and cryopreserved sperm (B–F). E) Cryopreservation-induced cellular injuries to the dorsal anterior plasma membrane in C57BL/6J mouse sperm. F) The elements on a larger scale of cryopreservation-induced cellular injuries to the dorsal anterior plasma membrane. Cryopreservation-induced cellular injuries are indicated by a white arrow and white arrowheads. Scale bar = 5 μm.

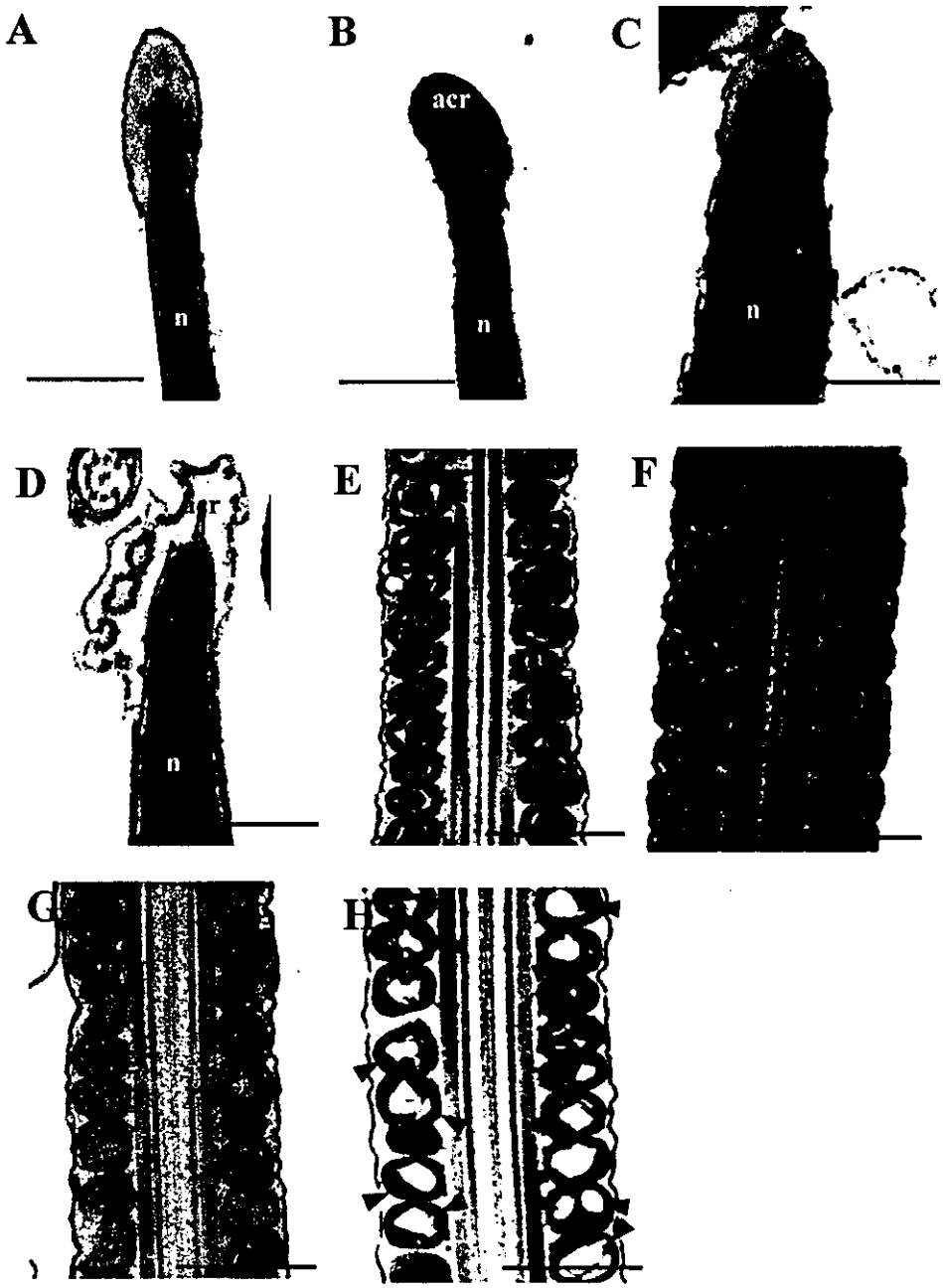

FIG. 5. Transmission electron micrographs of sperm from DBA/2N and C57BL/6J strains. Fresh sperm head (A) from DBA/2N and (C) from C57BL/6J and frozen-thawed sperm head (B) from DBA/2N and (D) from C57BL/6J. n, Nucleus; acr, acrosome. Mitochondria of the middle section from (E) fresh DBA/2N sperm, (F) frozen-thawed DBA/2N sperm, (G) fresh C57BL/6J sperm, and (H) frozen-thawed C57BL/6J sperm. Cryopreservation-induced cellular injuries are indicated by black arrowheads. Scale bar = 500 nm.

lytic enzymes (Fig. 5, A–C, indicating high electron density in the acrosome), but frozen C57BL/6J sperm had no acrosomal contents (Fig. 5D, indicating low electron density in the acrosome).

Furthermore, the mitochondria in the middle piece of frozen C57BL/6J spermatozoa had extremely variable and abnormal morphology compared with fresh sperm, whereas frozen DBA/2N spermatozoa had normal mitochondria (Fig. 5, E–H). The characteristic findings were mitochondria with an increased relative area of the matrix; thickening of the membrane, in particular the outer membranes; and swelling with loss of cristae (Fig. 5H, arrowheads).

Observation of Acrosomal Contents Using acr3-EGFP Transgenic Mice

In order to confirm the results of electron microscopy, the acrosomal content status using acr-3 EGFP transgenic mice sperm was examined (Fig. 6, A–D). As shown in Figure 6, A and B, in the case of fresh acr3-EGFP transgenic mouse spermatozoa, most sperm heads had acrosomal contents, as shown by green fluorescence (14.7%, the ratio of the sperm that does not have the acrosome contents). The profile of the fluorescence due to EGFP was identical to that of the acrosomal marker protein acrosin, indicating that EGFP was localized in the acrosome of acr3-EGFP mice spermatozoa.

However, in frozen acr-3 EGFP spermatozoa, EGFP-negative cells were observed with high frequency (Fig. 6, C and D, 50.9%, the ratio of the sperm that do not have the acrosome contents). The EGFP-negative cells indicated that the acrosomal contents had leaked out during cryotreatment. These results demonstrate that most frozen sperm in C57BL/6J background mice had no acrosomal contents.

TABLE 1. In vitro fertilization of zona-intact oocytes and zona-free oocytes by frozen spermatozoa.

State of oocytes	No. of males examined	No. of oocytes examined	No. (%) of eggs fertilized	
			Monospermic	Polyspermic
Zona-intact oocytes	5	411	70 (17.0)	0 (0)
Zona-free oocytes	3	262	148 (56.5)	8 (3.0)

In Vitro Fertilization Using Zona-Free Oocytes

To determine the effects of the freezing injury, sperm penetration of zona-free oocytes was examined. When frozen-thawed C57BL/6J sperm were used to inseminate zona-free oocytes, the fertilization rate was higher than for intact oocytes (56.5% vs. 17.0%; Table 1). In addition, when frozen-thawed C57BL/6J sperm were used to inseminate intact oocytes, the fertilization rate was low, but cryopreserved C57BL/6J sperm had the ability to bind to the zona pellucida but not to penetrate it.

DISCUSSION

Mouse sperm have proven to be more difficult to cryopreserve than other mammalian sperm. Difficulties in reproducing the original results [10–13] inspired modifications [23–25] to protocols to make freezing generally more reliable, but these are still not equally successful for all mouse strains. For example, the problem of the decreased fertilizing ability of frozen inbred mouse sperm, especially the C57BL/6J strain, is well known. Sherman and Liu [26] reported cryoinjury to cryopreserved mouse spermatozoa. They used only dimethyl sulfoxide as the cryoprotectant agent, whereas the standard method used 18% raffinose/3% skim milk cryoprotectant solution. Thus, a paucity of material is available on the causes of decreased fertilizing ability during cryotreatment, particularly cryobiology studies.

In this study, we found that the fertilization rate and sperm motility are not related in mouse spermatozoa (Figs. 1 and 2). Furthermore, in the case of frozen C57BL/6J spermatozoa, the percentage of damaged spermatozoa was 83.7% in total (Fig. 4). On the other hand, over 90% of frozen DBA/2N spermatozoa were intact. These observations suggest that cryopreservation-induced cellular injury is a potential cause of low fertilization. Quinn et al. [27] reported that freezing caused profound changes in the appearance of the acrosome in the majority of ram spermatozoa. In agreement with these results, we observed an abnormal acrosome in frozen C57BL/6J spermatozoa (Figs. 5 and 6). We also found that cryoinjury was localized to the dorsal anterior plasma membrane of the sperm head (Fig. 5). The proteins required for acrosome reaction are expressed in the rostral head region [28, 29].

Quinn et al. [27] also observed that in the midpieces changes occurred in the matrix of the mitochondria making up the mitochondrial sheath, the matrix appeared lighter in frozen spermatozoa than fresh spermatozoa, and loss of protein from the midpieces was confirmed histochemically. Imai et al. [30] reported that infertile human males with phospholipid hydroperoxidase glutathione peroxidase (PHGPx) defective spermatozoa accounted for about 10% of the total number of infertile males examined and for 35% of infertile males with oligoasthenozoospermia. The mitochondria in the midpiece of PHGPx-negative human spermatozoa have abnormal morphology: swollen, with loss of cristae. This phenotype is very similar to the mitochondrial

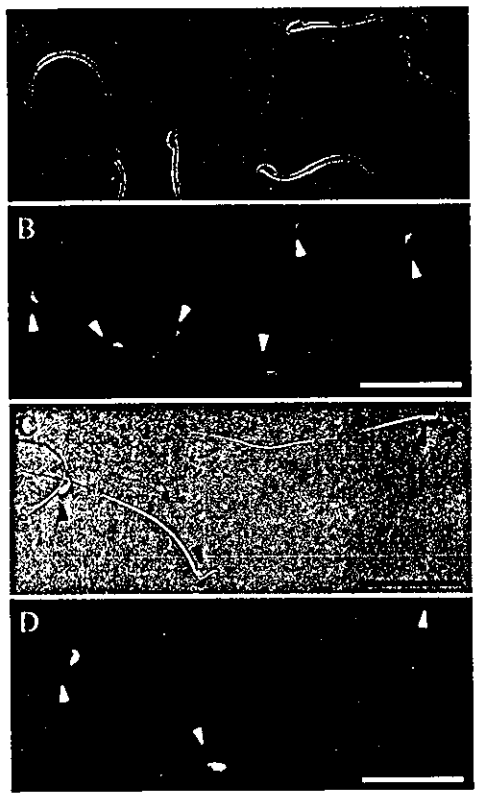

FIG. 6. Acrosomal contents status assay using acr3-EGFP transgenic mice. Sperm of the acr3-EGFP mouse as viewed by Hoffman modulation contrast microscopy (**A**, fresh; **C**, frozen-thawed) for EGFP expression under long-wavelength (480 nm) UV light (**B**, fresh; **D**, frozen-thawed). Arrowheads indicate the sperm head. Scale bar = 25 μm.

cellular injury of frozen C57BL/6J spermatozoa (Fig. 5). Additionally, although there was no significant difference among the motilities of cryopreserved sperm of DBA/2N, BALB/cA, and C57BL/6J after thawing (Fig. 2), in this study the rate of spermatozoa with high progressive motility was lower for C57BL/6J than for DBA/2N and BALB/cA under visual examination (data not shown). Thus, it appears that a defect in the mitochondria of frozen spermatozoa may be closely linked to lost fertilizing ability and high progressive motility.

Moreover, in the fluorescent study we found that the acrosome contents were missing from frozen acr3-EGFP mouse (C57BL/6J background) spermatozoa. The acrosome contents are vital proteins for passage through the zona pellucida surrounding an oocyte at fertilization, especially acrosin. The EGFP indicator expressed the same region as acrosin in the acrosome of frozen acr3-EGFP spermatozoa lost during cryotreatment (Fig. 6). In agreement with the results above, Müller et al. [31] reported that the plasma membrane of the acrosome was changed and the acrosomal contents were reduced in frozen ram spermatozoa. We demonstrated previously that the fertilization rate of C57BL/6J frozen spermatozoa could be increased by in vitro fertilization with oocytes subjected to partial dissection of the zona pellucida [16]. In this study, a relatively high fertilization rate was obtained when frozen C57BL/6J spermatozoa were used to inseminate zona-free oocytes. This knowledge and these results suggest that frozen C57BL/6J spermatozoa lost the ability to penetrate the zona pellucida as the result of decreased acrosome contents.

In conclusion, this study strongly suggests that the low fertilizing ability of frozen C57BL/6J spermatozoa resulted

from injury to the head and tail caused by freezing and thawing. The acrosome of frozen C57BL/6J spermatozoa was damaged and their contents lost during cryotreatment. As a result, frozen C57BL/6J spermatozoa could not induce an acrosome reaction and could not penetrate the zona pellucida of the egg. Frozen C57BL/6J spermatozoa also lost essential motility for fertilization because of the damage to the mitochondria. Thus, the fertilizing ability of mouse spermatozoa was lost during cryotreatment.

This study provides new and important information to modify the cryopreservation method. However, from the results of these experiments, it is difficult to demonstrate how the cellular injury in spermatozoa, especially C57BL/6J spermatozoa, occurred after freezing and thawing, and further investigation is necessary.

ACKNOWLEDGMENTS

We wish to thank Dr. Katsuhiro Sato for SEM and TEM technical assistance. We also wish to thank Dr. Minesuke Yokoyama for generously donating the transgenic mouse, acr3-EGFP. In addition, the encyclopedic knowledge of Dr. Shuichi Yamada about acr3-EGFP mice was gratefully appreciated.

REFERENCES

1. Bedell MA, Largaespada DA, Jenkins NA, Copeland NG. Mouse models of human disease. Part II: recent progress and future directions. Genes Dev 1997; 11:11–43.
2. Simpson EM, Linder CC, Sargent EE, Davisson MT, Mobraaten LE, Sharp JJ. Genetic variation among 129 substrains and its importance for targeted mutagenesis in mice. Nat Genet 1997; 16:19–27.
3. Hrabe de Angelis M, Balling R. Large scale ENU screens in the mouse: genetics meets genomics. Mutat Res 1998; 400:25–32.
4. Brown SD, Nolan PM. Mouse mutagenesis—systematic studies of mammalian gene function. Hum Mol Genet 1998; 7:1627–1633.
5. Knight J, Abbott A. Full house. Nature 2002; 417:785–786.
6. Marschall S, Hrabe de Angelis M. Cryopreservation of mouse spermatozoa: double your mouse space. Trends Genet 1999; 15:128–131.
7. Marschall S, Huffstadt U, Balling R, Hrabe de Angelis M. Reliable recovery of inbred mouse lines using cryopreserved spermatozoa. Mamm Genome 1999; 10:773–776.
8. Critser JK, Russell RJ. Genome resource banking of laboratory animal models. Inst Lab Anim Resour J 2000; 41:183–186.
9. Yokoyama M, Akiba H, Katsuki M, Nomura T. Production of normal young following transfer of mouse embryos obtained by in vitro fertilization using cryopreserved spermatozoa. Jikken Dobutsu 1990; 39: 125–128.
10. Tada N, Sato M, Yamanoi J, Mizorogi T, Kasai K, Ogawa S. Cryopreservation of mouse spermatozoa in the presence of raffinose and glycerol. J Reprod Fertil 1990; 89:511–516.
11. Okuyama M, Isogai S, Saga M, Hamada H, Ogawa S. In vitro fertilization (IVF) and artificial insemination (AI) by cryopreserved spermatozoa in mouse. J Fertil Implant 1990; 7:116–119.
12. Nakagata N, Takeshima T. High fertilizing ability of mouse spermatozoa diluted slowly after cryopreservation. Theriogenology 1992; 37: 1283–1291.
13. Nakagata N. Use of cryopreservation techniques of embryos and spermatozoa for production of transgenic (Tg) mice and for maintenance of Tg mouse lines. Lab Anim Sci 1996; 46:236–238.
14. Thornton CE, Brown SD, Glenister PH. Large numbers of mice established by in vitro fertilization with cryopreserved spermatozoa: implications and applications for genetic resource banks, mutagenesis screens, and mouse backcrosses. Mamm Genome 1999; 10:987–992.
15. Nakagata N. Cryopreservation of mouse spermatozoa. Mamm Genome 2000; 11:572–576.
16. Nakagata N, Okamoto M, Ueda O, Suzuki H. Positive effect of partial zona-pellucida dissection on the in vitro fertilizing capacity of cryopreserved C57BL/6J transgenic mouse spermatozoa of low motility. Biol Reprod 1997; 57:1050–1055.
17. Wakayama T, Whittingham DG, Yanagimachi R. Production of normal offspring from mouse oocytes injected with spermatozoa cryopreserved with or without cryoprotection. J Reprod Fertil 1998; 112:11–17.
18. Hogan B, Beddington R, Costantini F, Lacy E. Manipulating the Mouse Embryo, 2nd ed. New York: Cold Spring Harbor Laboratory Press; 1994:173–178.
19. Nakanishi T, Ikawa M, Yamada S, Parvinen M, Baba T, Nishimune Y, Okabe M. Real-time observation of acrosomal dispersal from mouse sperm using GFP as a marker protein. FEBS Lett 1999; 449: 277–283.
20. Nakanishi T, Ikawa M, Yamada S, Toshimori K, Okabe M. Alkalinization of acrosome measured by GFP as a pH indicator and its relation to sperm capacitation. Dev Biol 2001; 237:222–231.
21. Quinn P, Kerin JF, Warnes GM. Improved pregnancy rate in human in vitro fertilization with the use of a medium based on the composition of human tubal fluid. Fertil Steril 1985; 44:493–498.
22. Sztein JM, Farley JS, Mobraaten LE. In vitro fertilization with cryopreserved inbred mouse sperm. Biol Reprod 2000; 63:1774–1780.
23. Dewit M, Marley WS, Graham JK. Fertilizing potential of mouse spermatozoa cryopreserved in a medium containing whole eggs. Cryobiology 2000; 40:36–45.
24. Penfold LM, Moore HD. A new method for cryopreservation of mouse spermatozoa. J Reprod Fertil 1993; 99:131–134.
25. Songsasen N, Leibo SP. Cryopreservation of mouse spermatozoa. I. Effect of seeding on fertilizing ability of cryopreserved spermatozoa. Cryobiology 1997; 35:240–254.
26. Sherman JK, Liu KC. Ultrastructure before freezing, while frozen, and after thawing in assessing cryoinjury of mouse epididymal spermatozoa. Cryobiology 1982; 19:503–510.
27. Quinn PJ, White IG, Cleland KW. Chemical and ultrastructural changes in ram spermatozoa after washing, cold shock and freezing. J Reprod Fertil 1969; 18:209–220.
28. Breitbart H, Naor Z. Protein kinases in mammalian sperm capacitation and the acrosome reaction. Rev Reprod 1999; 4:151–159.
29. Snell WJ, White JM. The molecules of mammalian fertilization. Cell 1996; 85:629–637.
30. Imai H, Suzuki K, Ishizaka K, Ichinose S, Oshima H, Okayasu I, Emoto K, Umeda M, Nakagawa Y. Failure of the expression of phospholipid hydroperoxide glutathione peroxidase in the spermatozoa of human infertile males. Biol Reprod 2001; 64:674–683.
31. Müller K, Pomorski T, Muller P, Herrmann A. Stability of transbilayer phospholipid asymmetry in viable ram sperm cells after cryotreatment. J Cell Sci 1999; 112:11–20.

J Toxicol Pathol 2004; 17: 105–112

Original

Effects of a Hemizygous Deletion of Mouse Chromosome 2 on the Hematopoietic and Intestinal Tumorigenesis

Yumiko Nitta[1], Kazuko Yoshida[2], Naomi Nakagata[3], Toshihide Harada[4], Fumiko Ishizaki[5], Kohsaku Nitta[6], and Mikinori Torii[7]

[1]International Radiation Information Center, Research Institute for Radiation Biology and Medicine, Hiroshima University, Kasumi, Minami-Ku, Hiroshima 734–8553, Japan
[2]Environmental and Toxicological Sciences Research Group, National Institute for Radiological Science, Anagawa, Inage-Ku, Chiba 263–8555, Japan
[3]Division of Reproductive Engineering, Institute of Resource Development and Analysis, Kumamoto University, 2–2–1 Honjo, Kumamoto 860–0811, Japan
[4]Third department of Internal Medicine, School of Medicine, Hiroshima University, 1–2–3 Kasumi, Minamiku, Hiroshima 734–8551, Japan
[5]Hiroshima Prefecture College of Health Science, 1–1 Gakuennmachi, Mihara, Hiroshima 723–0053, Japan
[6]Ootani Rehabilitation Hospital, 1970 Kakiura, Ohgakicho, Saiki, Hiroshima 737–2211, Japan
[7]Developmental of Research Laboratories, Shionogi Co. Ltd., 3–1–1 Futaba, Toyonaka, Osaka 561–0825, Japan

Abstract: Allelic loss of chromosome 2 is associated with radiation-induced murine acute myeloid leukemia. However, the gene, which contributes mainly to the leukemogenesis in a tumor suppression manner, has not been identified, yet. Expecting predisposition to acute myeloid leukemia, a radiation leukemogenesis experiment was performed with $Pax6^{Sey3H}$, one of the small eye mutants. Deletion mapping of $Pax6^{Sey3H}$ indicated that the deleted segment extended from 106.00 to 111.47 Mb from the centromere with a length of 5.47 Mb on chromosome 2. Six known and seventeen novel genes were located in the segment. $Pax6^{Sey3H}$ mutants crossed back into C3H/He did not develop hematopoietic tumors spontaneously, but they did after exposure to γ-rays. The final incidence of hematopoietic tumor in mutants (45.2%) was higher than that in normal sibs (26.2%), and the survival curve of mutants shifted toward the left ($p<0.05$ by the Cox-Mantel test). Mutants developed intestinal tumors spontaneously with long latency as well as showing abnormality in the Wirsung's duct from young ages. Congenital deletion of the 5.47 Mb segment at the middle region on chromosome 2 alone did not trigger hematopoietic tumors, however, the deletion promoted the development of hematopoietic tumors initiated by radiation. The deletion developed intestinal tumors spontaneously. Radiation exposure at 10 weeks of age did not contribute to the intestinal tumorigenesis. (J Toxicol Pathol 2004; 17: 105–112)

Key words: chromosome deletion, $Pax6^{Sey3H}$, Wilsung's duct, intestinal tumor, radiation

Introduction

It is well known that leukemia occurs more frequently among atomic bomb survivors than in the general population[1–3]. Clinical, cytogenetic and molecular-genetic examinations indicate that complex chromosome abnormalities without specific types of translocation and high incidence of genetic instability of leukemic cells are characteristic of radiation-related acute myeloid leukemia in humans[4].

Received: 13 January 2004, Accepted: 13 April 2004
Mailing address: Yumiko Nitta, International Radiation Information Center, Research Institute for Radiation Biology and Medicine, Hiroshima University, Kasumi, Minami-Ku, Hiroshima 734–8553, Japan
TEL & FAX: 81-82-257-5877
E-mail: yumiko@hiroshima-u.ac.jp

To clarify the mechanism of leukemogenesis, an experimental model is useful. Hayata et al. reported the high susceptibility of C3H/He mice to myeloid leukemia and the consistent occurrence of chromosome 2 deletions in mouse myeloid leukemias[5,6]. Since this publication, three independent articles have demonstrated the deletion of chromosome 2 in mouse radiation-induced acute myeloid leukemias[7–9]. Interestingly, the length of these three deleted regions was different, 6.5 cM, 1.0 cM and 4.6 cM for each reference, respectively, but they involved *Wt1* and *Pax6* genes commonly.

The WAGR (*Wilms'* tumor, aniridia, genitourinary anomalies, mental retardation) syndrome is one of the well known congenital disorders, the patients of which have simultaneous deletion of *PAX6* and *WT1* (OMIM#194072). The mouse small eye mutant, $Pax6^{Sey1H}$ is the animal model of the WAGR syndrome, and is characterized by the

Table 1. Tumor Spectrum of the *Pax6*^{Sey3H} Mice

Genetic background (%)	C3H/He (93.5≤)				JF1 (50.0)			
Treatment	None		Co-60		None		Co-60	
Genotype[a]	+/del	+/+	+/del	+/+	+/del	+/+	+/del	+/+
Number of mice examined[b]	14	17	31	42	16	19	30	28
Number of mice bearing tumors	5	5	25	32	2	0	22	12
Number of tumors observed	5	5	28	33	2	0	25	12
Hematopoietic systems (%)	0	1 (5.9)	14 (45.2)[d,e]	11 (26.2)[f]	0	0	3 (10.0)	2 (7.1)
Intestinal tract (%)	4 (28.6)	0	8 (25.8)	0	0	0	6 (20.0)[f]	1 (3.6)
Others[c]	1	4	6	22	2	0	16	9

a: +/del; hemizygous mutants, +/+; normal sibs.
b: Sex ratios (female/male) were 6/8, 10/7, 19/12 and 18/24 for (C3H × *Pax6*^{Sey3H}) groups, and 8/8, 10/9, 17/13 and 15/13 for (JF1 × *Pax6*^{Sey3H}) groups.
c: Others included tumors in the liver, lung, pancreas, ovary and soft tissue.
d: $p<0.01$ when compared to non-treated normal sibs by the comparison of ratios of tumors.
e: $p<0.01$ when compared to γ-irradiated normal sibs by the chi-square test.
f: $p<0.01$ when compared to non-treated normal sibs by the chi-square test.

cytogenetic deletion at the two genes' loci and by the small eye phenotype[10]. It is of great interest whether the congenital deletion of *Wt1* and *Pax6* predisposes mice to acute myeloid leukemia or not. If the deletion mutants developed acute myeloid leukemia, and if any mutation was found in the monoallelic genes of myeloid leukemia cells, it might be possible to identify the gene responsible for leukemogenesis.

We tested the susceptibility of *Pax6*^{Sey3H} to radiation using the established system for the induction of acute myeloid leukemia[11], and the effect of the hemizygous deletion of mouse chromosome 2 on radiation-induced hematopoietic tumorigenesis including myeloid leukemogenesis. As the *Pax6*^{Sey3H} mutant was found to develop not only intestinal tumors, but also a malformation of the Wirsung's duct unexpectedly, these two phenotypes are discussed with regard to the deletion of genes.

Materials and Methods

Mice

Frozen embryos of the *Pax6*^{Sey3H} hemizygous mutant were purchased from MRC (Harwell, OXON, UK), and the mutant has been maintained by crossing with C3H/He (Charles River Japan Inc.)[13]. Offspring were used for the following two experiments. F1 hybrids backcrossed with C57BL/6N, BALB/C (Charles River Japan Inc.) or JF1 (National Institute of Genetics, Mishima, Japan) were for the deletion mapping. The *Pax6*^{Sey3H} mice of the 3rd and 4th generations crossed back onto C3H/He (C3H × *Pax6*^{Sey3H}), and the F1 hybrid between *Pax6*^{Sey3H} and JF1 (JF1 × *Pax6*^{Sey3H}) were for the tumorigenesis experiment. This mutant was endowed with high fertility and viability, which were essential factors to complete carcinogenesis experiments using any mutant.

Animals were housed less than 5 in a plastic cage with soft wood chips for bedding in an air conditioned room (temperature 22 ± 2°C) with a 12-h light/dark cycle. Food and water were available *ad libitum*. Animal studies were carried out under the guidance issued by the Research Institute for Radiation Biology and Medicine in Responsibility in the Use of Animals for Research.

Genotyping the mutant

Genuine DNA was prepared from the tail tips using a DNA rapid extraction kit (Qiagen, Hilden, Germany). The single strand length polymorphism markers used were Massachusetts Institute of Technology (Mit) markers. The marker set used was: *D2Mit354, D2Mit219, D2Mit435, D2Mit183, D2Mit436, D2Mit220, D2Mit126, D2Mit14, D2Mit15, D2Mit302, D2Mit253, D2Mit186, D2Mit351, D2Mit350, D2Mit386, D2Mit303, D2Mit141, D2Mit221, D2Mit385, D2Mit184, D2Mit437, D2Mit249, D2Mit251, D2Mit250, D2Mit477, D2Mit333, D2Mit42, D2Mit99, D2Mit442, D2Mit387, D2Mit185, D2Mit128, D2Mit100, D2Mit206, D2Mit211, D2Mit58, D2Mit480, D2Mit482, D2Mit207, D2Mit102, D2Mit103, D2Mit398, D2Mit278, D2Mit487, D2Mit304, D2Mit224, D2Mit258, D2Mit78, D2Mit353* and *D2Mit13*. The sequence was obtained from the Whitehead Institute for Biomedical Research/MIT Center for Genome Research (http://www.genome.wi.mit.edu/), and their primers were obtained from Greiner Bio-One Ltd, Japan. The cycling conditions for the PCR were 40 × (1 min at 95°C, 1 min at 42°C, and 2 min at 72°C)[12]. Aliquots of the 10 μl of products were separated by electrophoresis on 3% agarose gel.

Tumorigenicity test

Whole body exposure to γ-irradiation emitted from a ^{60}Co source (Shimadzu, Japan) was performed at the age of 10 weeks. The exposure was a single dose of 3.0 Gy at a rate of 68.7 cGy/min[11]. The number of mice used is shown in Table 1. Their health was checked every weekday morning. The tumorigenicity has been observed up to 24 months of age.

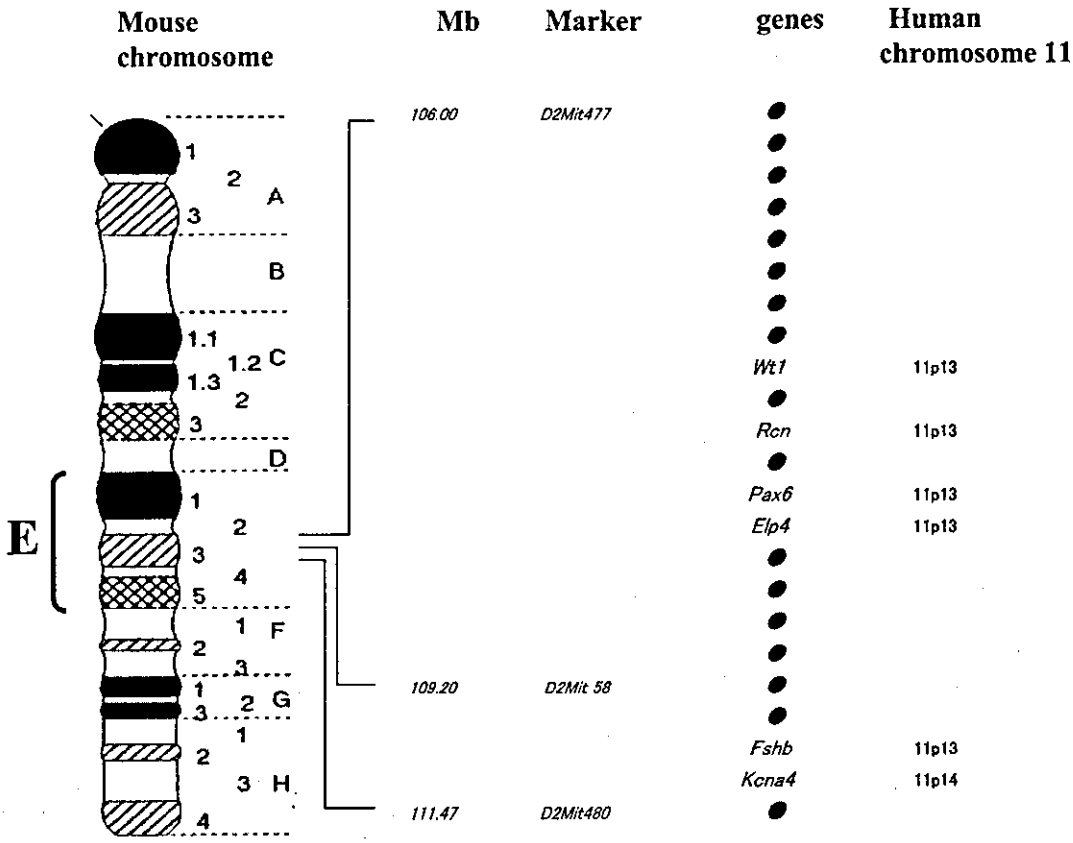

Fig. 1. Cytogenetic map of chromosome 2 combined with the genomic map of the deleted segment of $Pax6^{Sey3H}$. Base number was counted from the centromere. The symbol (●) indicates the novel gene.

Histopathological analysis

Mice were sacrificed when moribund, exhibiting anemia with palpable spleens or at the ages of termination, 24 months. Organs and tumor tissues were fixed in 10% phosphate buffered formalin, dehydrated with alcohol, embedded in paraffin wax, sectioned 4 μm thick, stained with hematoxylin and eosin (H&E), and observed pathologically. Intestines from stomach to colon were sliced into serial sections 4 μm thick, and three serial sections were mounted per glass slide. Sections were stained with H&E for every five glass slides in order to examine the tumor multiplicity. For the observation of the Wirsung's duct at 1 week of age, the intestines of five each of mutants and normal sibs were observed in the same manner.

A standard avidin-biotin complex technique[13] was performed to detect the peroxidase in the hematopoietic tumor cells in the liver. Polyclonal antibodies to peroxidase (MBL Inc., Japan) were used as the primary antibody at a titer of 1:1000.

Statistical analysis

Survival ratios were calculated by the Kaplan-Meier method[14]. The difference between the survival curves was evaluated using the log-rank test and Cox-Mantel test. Incidences of tumors at the age of 24 months were compared statistically by the chi-square test or by a *t*-test.

Results

Deletion region of mutants

The deleted segment was between markers *D2Mit477* and *D2Mit480* (Fig. 1). The interval was 5.47 Mb between 106.00 Mb and 111.7 Mb from the centromere, in which the six known, *Wilms'* tumor 1 (*Wt1*), Reticulocarbin (*Rcn*), Paired box gene 6 (*Pax6*), Elongation protein homolog 4 (*Elp4*), Follicular stimulation hormone beta (*Fshb*) and Potassium channel voltage-gated shaker-related super family 4 (*Kcna4*), and 17 novel genes located (http://www.ensembl.org/Mus_musculus/geneview). The deleted segment of $Pax6^{Sey3H}$ was found to be longer than that previously reported (http://mrcseq.har.mrc.ac.uk/chr2map.html) by 2.27 Mb. Five genes, *Fshb*, *Kcna4*, and three novel genes, located within the segment (Fig. 1).

Hematopoietic tumorigenesis of the mutant

(C3H × $Pax6^{Sey3}$) mutants did not develop hematopoietic tumors spontaneously but did when γ-irradiated ($p<0.01$ by the chi-square test) (Table 1). The development of myeloid leukemia was radiation specific ($p<0.01$ by the chi-square test) (Table 2). The cumulative

Table 2. Hematopoietic Tumors

Genetic background (%)	C3H/He (93.5≤)				JF1 (50.0)			
Treatment	None		Co-60		None		Co-60	
Genotype (number of mice)	+/del (14)	+/+ (17)	+/del (31)	+/+ (42)	+/del (16)	+/+ (19)	+/del (30)	+/+ (28)
Number of tumors observed (%)	0	1 (5.9)	14 (45.2)	11 (26.2)	0	0	3 (10.0)	2 (7.1)
Thymic lymphoma (%)	0	0	3 (9.7)	1 (2.4)	0	0	1 (3.3)	0
Non-thymic lymphoma (%)	0	1 (5.9)	3 (9.7)	0	0	0	0	1 (3.6)
Myeloid leukemia (%)	0	0	8 (25.8)[a]	9 (21.4)[a]	0	0	2 (6.7)	1 (3.6)
Erythroleukemia (%)	0	0	0	1 (2.4)	0	0	0	0

a: p<0.01 when compared to non-treated normal sibs by the comparison of ratios of tumors.

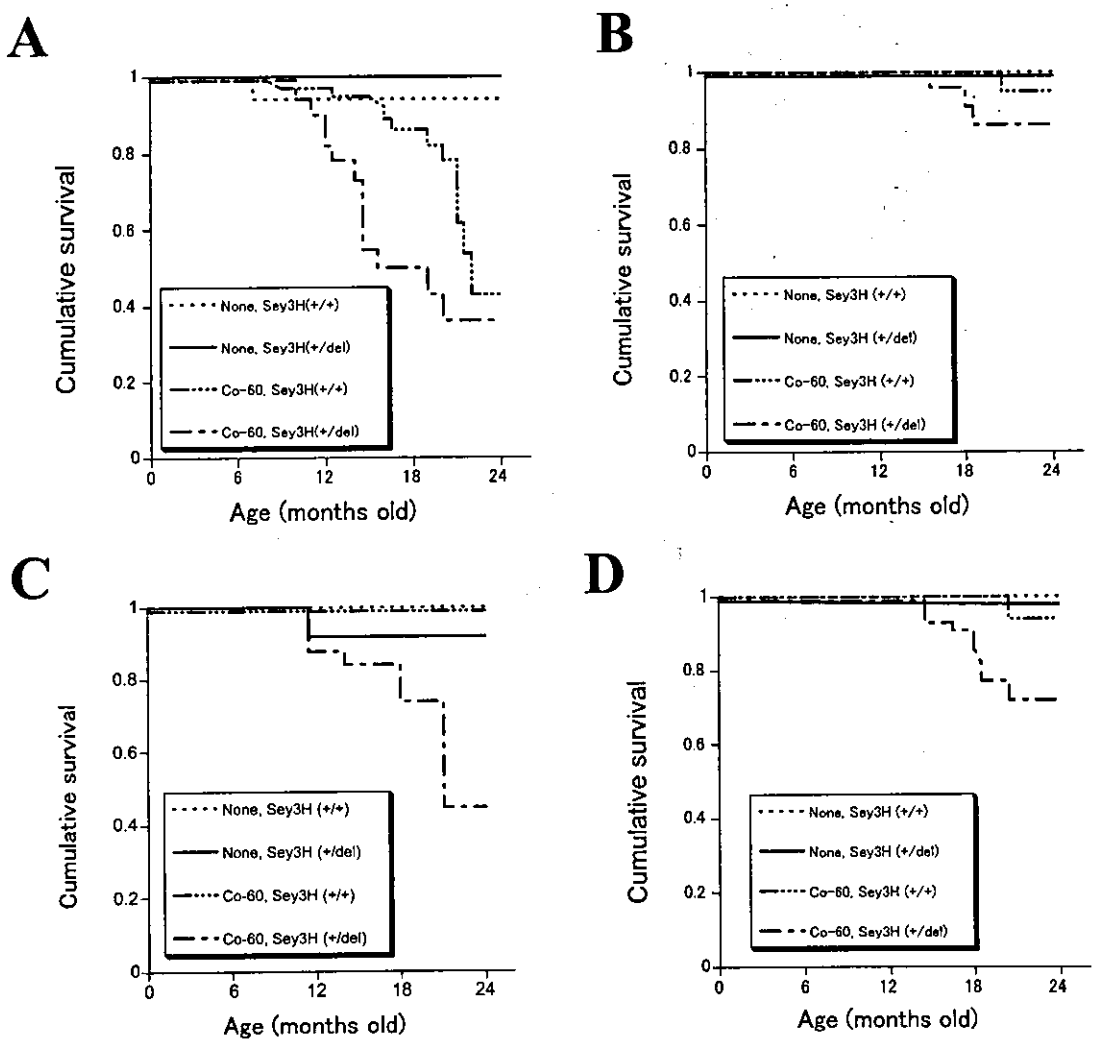

Fig. 2. **A**: Kaplan-Meier survival curves of (C3H × *Pax6*^{Sey3H}) mice with the parameter of hematopoietic tumors. Difference between the curve of γ-irradiated mutants (— · —) and that of γ-irradiated normal sibs (— · · —) was significant by the log-rank test (p<0.01).
B: Kaplan-Meier survival curves of (JF1 × *Pax6*^{Sey3H}) mice with the parameter of hematopoietic tumors.
C: Kaplan-Meier survival curves of (C3H × *Pax6*^{Sey3H}) mice with the parameter of intestinal tumors. Difference between the curve of γ-irradiated mutants (— · —) and that of γ-irradiated normal sibs (— · · —) was significant by the log-rank test and Cox-Mantel test (p<0.01).
D: Kaplan-Meier survival curves of (JF1 × *Pax6*^{Sey3H}) mice with the parameter of intestinal tumors. Difference between the curve of γ-irradiated mutants (— · —) and that of γ-irradiated normal sibs (— · · —) was significant by the log-rank test and the Cox-Mantel test (p<0.01).

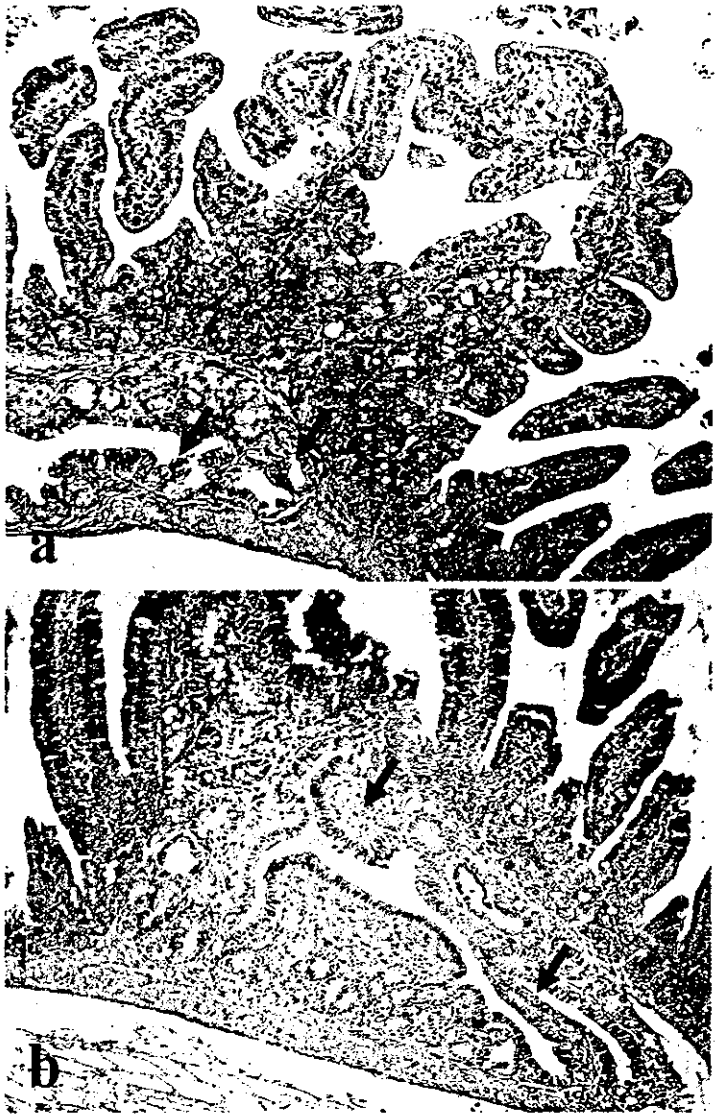

Fig. 3. Histopathology of the Wirsung's duct.
a: Epithelial cell proliferation (arrow) of Wirsung's duct and oblongation of the vili at the duodenal papilla of a non-treated (C3H × *Pax6*^{Sey3H}) mutant. H&E staining. (× 100 in original magnification).
b: Intraductal papillary proliferation of the epithelium of Wirsung's duct (arrow) with partial thickening of the duodenal duct of a non-treated (C3H × *Pax6*^{Sey3H}) mutant. H&E staining. (× 100 in original magnification).

survival curve of the mutants bearing hematopoietic tumors shifted toward the left when compared to that of the normal sibs (Fig. 2a).

Spontaneous hematopoietic tumors were not observed in (JF1 × *Pax6*^{Sey3H}) mutants (Table 1). Incidences of hematopoietic tumors were very low in the γ-irradiated groups (Table 2). The cumulative survival ratios with the parameter of hematopoietic tumors were kept high by the end of the experiment (Fig. 2b).

Intestinal tumorigenesis of the mutant

(C3H × *Pax6*^{Sey3H}) mutants developed intestinal tumors spontaneously, but the incidence of intestinal tumors was not increased by radiation (Table 1). The cumulative survival curves with the parameter of intestinal tumors showed statistically significant acceleration of tumor development in γ-irradiated mutants ($p<0.01$ by the log-rank test and by the Cox-Mantel test) (Fig. 2c).

(JF1 × *Pax6*^{Sey3H}) mutants developed intestinal tumors when exposed to γ-rays ($p<0.01$ by the chi-square test) (Table 1). The mean latency of intestinal tumors was longer than that of hematopoietic tumors ($p<0.01$ by a *t*-test) (Table 3). Survival curves drawn by the parametric Kaplan-Meier method showed statistically significant acceleration of the tumor development in γ-irradiated mutants ($p<0.01$ by the log-rank test and by the Cox-Mantel test) (Fig. 2d).

Histopathology

Pax6^{Sey3H} mutants showed abnormalities in the Wirsung's duct. Most parts of the Wirsung's duct were composed of a single layer of tall columnar epithelial cells and goblet cells. The papillary protrusion with the proliferation of ductal epithelium was arranged in aged mutants (Figs. 3-a and b). The hypertrophied Wirsung's duct occasionally pushed up the duodenal villi. Epithelial proliferation of the Wirsung's duct was observed from 1 week of age in all mutants examined.

Intestinal tumors found in the mutants were adenomas

Table 3. Tumor Latencies

Groups	Genetic background (%)	C3H/He (93.5≤)				JF1 (50.0)			
	Treatment	None		Co-60		None		Co-60	
	Genotype	+/del	+/+	+/del	+/+	+/del	+/+	+/del	+/+
Tumor latency[a]	Hematopoietic tumor	–	–	348.3 ± 101.0	472.1 ± 119.2	–	–	320.3 ± 63.3[b]	356
(days, mean ± SD)	Intestinal tumor	295	–	401.5 ± 134.5	–	–	–	456.3 ± 49.0	568

a: Days between the γ-irradiation and the sacrifice before 24 months of age.
b: $p<0.01$ when compared to the value of intestinal tumor by a *t*-test.

Table 4. Intestinal Tumors

Genetic background (%)	C3H/He (93.5≤)				JF1 (50.0)			
Treatment	None		Co-60		None		Co-60	
Genotype (number of mice)	+/del (14)	+/+ (17)	+/del (31)	+/+ (42)	+/del (16)	+/+ (19)	+/del (30)	+/+ (28)
Number of tumors observed (%)	4 (28.6)	0	8 (25.8)	0	0	0	6 (20.0)	1 (3.6)
Forestomach squamous cell carcinoma	0	0	6	0	0	0	3	1
Duodenum, tubular adenoma	3	0	0	0	0	0	2	0
Duodenum, tubular adenocarcinoma	0	0	2	0	0	0	1	0
Ileum,tubular adenocarcinoma	1	0	0	0	0	0	0	0

Table 5. Genes Contributed for the Tumor Development in the Alimentary Tract

Gene symbol	Gene name	Tumor site	Pathology	Reference
Apc	adenomatosis polyposis coli	small intestine	adenoma	28
Apc + Mlh1	*Apc*, *E. Coli* mutL homolog 1	stomach, intestine	adenoma	29
Apc + Mon1	*Apc*, Modifier of *Min 1*	stomach, intestine	adenoma	30
Apc + Mon2	*Apc*, Modifier of *Min 2*	stomach, intestine	adenoma	31
Apc + Msh2	*Apc*, *E. Coli* mutS homolog2	small intestine	adenoma	32
Apc + Prkdc	*Apc*, protein kinase DNA activated catalytic polypeptide	small intestine	adenoma	33
Apc + Trp53	*Apc*, transformation related protein 53	illeocecal junction, small intestine	adenoma	34
Apc + Blm	*Apc*, bloom syndrome homolog	small intestine	adenoma	35
Catnb + Krt1	catenin beta, keratin gene complex 1 acidic	small intestine	adenoma	36
Cdkn1b + Cdkn2c	cyclin dependent kinase inhibitor 1b, 2c	small intestine, stomach (neuroendocrine cells)	adenoma, hyperplasia	37
Cdkn1b + Pten	*Cdkn1b*, phosphatase and tensin homolog	small intestine	adenoma	38
Ahr	aryl-hydrocarbon receptor	stomach (glandular)	hyperplasia	39
Cdx2	caudal type homeo box 2	stomach, intestine	adenoma	40
Madh4	*Drosophila MAD* homolog 4	small intestine, stomach (glandular)	adenoma, hyperplasia	41
Msh3	*E.Coli mutS* homolog 3	small intestine	adenoma	42
Muc2	mucin 2	small intestine	adenoma	43
Runx3	runt related transcription factor 3	stomach (glandular)	hyperplasia	44

and adenocarcinomas at the junction of the pylorus to duodenum, duodenum or ileum, and squamous cell carcinomas developed in the forestomach (Table 4).

Discussion

In leukemogenesis, chromosome translocations (CTs) causing deregulated expression of oncogenes or the generation of fusion genes are the most frequent event, followed by the deletion of tumor suppressor genes, and by the point mutation of responsible genes[15,16]. Two CTs activating the oncogenes, t(14;18)(q32;q21) and t(8;14)(q24;q32), and five CTs forming the fusion-genes, t(2;5)(p23;q35), t(9;22)(q34;q11), t(4;11)(q21;q23), t(15;17)(q22;q11), t(8;21)(q22;q22) were detected in the peripheral blood cells of healthy individuals (17–23, respectively). This indicates that CTs associated with malignant tumors have already taken place in the non-neoplastic cells. Studies on monozygotic twins with concordant leukemia[16] and screening of the two CTs on umbilical cord bloods[23] showed that the genomic heterogeneity of the hematopoietic stem cells started during the embryogenesis. Among CTs observed in healthy individuals, only the *Myc*-activating CT, T(12;15), the murine counterpart of the human t(8;14)(q24;q32), has occurred spontaneously in mice to develop plasmacytoma[24]. Multiple mutations must be required for the stem cells to become clonogenic as hematopoietic neoplasms, however, it

is not clear whether hierarchy exists among the mutations or not.

A breakpoint cluster has been reported at 11p13 in human sporadic hematopoetic tumors; the inversion of chromosome11, inv(11)(p13; q23)[25] or the CT of t(11; 14)(p13; q11)[26] in acute lymphoblastic leukaemias. The existence of a breakpoint cluster at the syntenic site in mice has been proven by the establishment of small eye mutants[27]. Their phenotype of tumorigenicity with regard to hematopoietic tumors was tested. Our conclusion at the moment was that a congenital hemizygosity of the short segment of *Pax6*^{Sey3H} alone was not enough for developing hematopoietic tumors.

Spontaneous development of the intestinal tumors in *Pax6*^{Sey3H} was unique. There has been no report, in which any of the six known genes in the deleted segment associated with the intestinal tumors. Table 5 shows the genes, whose mutations develop intestinal tumors spontaneously with high frequency (over 50% of incidences) in mice[28–44]. Most of the genes are in the category of tumor suppressor genes[45]. One exception is the Caudal type homeobox 1 (*Cdx1*) gene encoding a transcription factor cognate of the *Drosophila* 'caudal' gene (OMIM#600746). The expression of *CDX1* in adult humans has been limited to the alimentary tract associated with gastric cancer[46]. This is one example of transcription factor genes contributing to the tumorigenesis of the intestine. The expression of the *Pax6*, another transcription factor gene, should be examined in the intestinal tumor cases.

Intestinal tumorigenesis was promoted by radiation, no matter how the age at exposure was not suitable for the induction of solid tumors. As the Wirsung's duct epithelium is differentiated by the regulation of *Pax6* during morphogenesis, the genomic dosage of *Pax6* may influence the proliferation of the epithelium and hypertrophy of the Wirsung's duct.

Acknowledgements: This work was supported by a grant from the Ministry of Education, Culture, Sports, Science and Technology (Tokyo, Japan) (Y.N., 1287092).

References

1. Ichimaru M and Ishimaru T. Leukenia and related disorders. Radiat Res (Suppl) 1975; **16**: 89–96.
2. Kodama K, Mabuchi K, and Shigenatsu I. A long-term cohot study of the atomic-bomb survivors. J Epidemiol (Suppl) 1996; **6**: S95–S105.
3. Pierce DA, Shimizu Y, Preston DL, Vaeeth M, and Mabuchi K. Studies of mortality of atomic bomb survivors. Report 12. Part I. Cancer: 1950–1990. Radiat Res 1996; **146**: 1–27.
4. Nakanishi M, Tanaka K, Shintani T, Takahashi T, and Kamada N. Chromosomal instability in acute myelocytic leukemia and myelodysplastic syndrome patients among atomic bomb survivors. J Radiat Res 1999; **40**: 159–167.
5. Hayata I, Ishihara T, Hirashima K, Sado T, and Yamagiwa J. Partial deletion of chromosome 2 in myeloid leukemias of irradiated C3H/He and RFM mice. J Natl Cancer Inst 1977; **63**: 843–848.
6. Hayata I, Seki M, Yoshida K, Hirashima K, Sado T, Yamagiwa J, and Ishihara T. Chromosomal aberrations observed in 52 mouse myeloid leukemias. Cancer Res 1983; **43**: 367–373.
7. Alexander BJ, Rasko JEJ, Morahan G, and Cook WD. Gene deletion explains both in vivo and in vitro generated chromosome 2 aberrations associated with murine myeloid leukemia. Leukemia 1995; **9**: 2009–2015.
8. Silver A, Moody J, Dunford R, Clark D, Ganz S, Bulman R, Boiuffler S, Finnon P, Meijne E, Kuiskamp R, and Cox R. Molecular mapping of chromosome 2 deletions in murine radiation-induced AML localizes a putative tumor suppressor gene to a 1.0cM region homologous to human chromosome segment 11p11~12. Genes Chromosome Cancer 1999; **24**: 95–104.
9. Rithidech K, Dunn JJ, Roe BA, Gorden R, and Cronkite EP. Evidence for two commonly deleted regions on mouse chromosome 2 in γ-ray-induced acute myeloid leukemic cells. Exp Hematol 2002; **30**: 564–570.
10. Hill RE, Favor J, Hogan BLM, Tom CC, Saunders GF, Handon IM, Prosser J, Jordan T, Hastie ND, and Van Heyningen V. Mouse small eye results from mutations in a paired-like homeobox-containing gene. Nature 1991; **354**: 522–525.
11. Seki M, Yoshida K, Nishimura M, and Nemoto K. Radiation-induced myeloid leukemia in C3H/HeNirsMs mice and the effect of predonizolone acetate on leukemogenesis. Radiat Res 1991; **127**: 146–155.
12. Nitta Y, Yoshida K, Tanaka K, Peters J, and Cattanach BM. The mouse small eye mutant, *Del (2)Sey3H* which deletes the putative tumor suppressor region of the radiation-induced acute myeloid leukemia is susceptible to radiation. In: Molecular Mechanisms for Radiation-induced Cellular Response and Cancer Development, K Tanaka, T Takabatake, K Fujikawa, T Matsumoto, F Sato (eds), Inst Environ Science, 136–142, 2002.
13. Nitta Y and Hoshi M. Relationship between oocyte apoptosis and ovarian tumors induced by high and low LET radiations in mice. Int J Radiat Biol 2003; **79**: 241–250.
14. Robinson CV and Upton AC. Competing-risk analysis of leukemia and nonleukemia mortality in X-irradiatewd, male RF mice. J Natl Cancer Inst 1978; **60**: 995–1007.
15. Bain BJ. An overview of translocation-related oncogenesis in the chronic myeloid leukemias. Acta Hematol 2002; **107**: 57–63.
16. Janz S, Potter M, and Rabkin CS. Lymphoma- and leukemia-associated chromosomal translocations in healthy individuals. Genes Chromosomes and Cancer 2003; **36**: 211–223.
17. Liu Y, Hernandez AM, Shibata D, and Cortopassi GA. BCL2 translocation frequrncy rises with age in humans. Proc Natl Acad Sci USA 1994; **91**: 8910–8914.
18. Muller JR, Janz S, Goedert JJ, Potter M, and Rabkin CS. Persistence of immunoglobulin heavy chain/c-myc recombination-positive lymphocyte clones in the blood of human immunodeficiency virus-infected homosexual men. Proc Natl Acad Sci USA 1995; **92**: 6577–6581.
19. Trumper L, Pfreundschuch M, Bonin FV, and Daus H. Detection of the t(2;5)-associated *NPM/ALK* fusion cDNA in peripheral blood cells of healthy individuals. Br J Hematol 1998; **103**: 1138–1144.

20. Eguchi-Ishimae M, Eguchi M, Ishii E, Miyazaki S, Ueda K, Kamada N, and Mizutani S. Breakage and fusion of the *TEL* gene in immature B lymphocytes induced by apoptogenic signals. Blood 2001; **97**: 737–743.
21. Bose S, Deininger M, Gora-Tyber J, Goldman JM, and Melo JV. The presence of typical and atypical *BCR/ABL* fusion genes in leukocytes of normal individuals. Blood 1998; **92**: 3362–3367.
22. Quina AS, Camerio P, Sa Da Costa M, Telhada M, and Parreira L. *PML-RARA* fusion transcripts in irradiated and normal hematopoietic cells. Genes Chromosomes Cancer 2001; **29**: 266–275.
23. Mori H, Colman SM, Xiao Z, Ford AM, Healy LE, Donaldson C, Hows JM, Navarrete C, and Greaves M. Chromosome translocations and covert leukemic clones are generated during normal fetal development. Proc Natl Acad Sci USA 2002; **99**: 8242–8247.
24. Potter M and Wiener F. Plasmacytomagenesis in mice: model of neoplastic development dependent upon chromosomal translocation. Carcinogenesis 1992; **13**: 1681–1697.
25. Raimondi SC, Frestedt JL, Pui CH, Downing JR, Head DR, Kersey JH, and Behm FG. Acute lymphoblastic leukemias with deletion of 11q23 or a novel inversion (11)(p13q23) lack *MLL* gene rearrangements and have favorable clinical features. Blood 1995; **86**: 1881–1886.
26. Foroni L, Boehm T, Lampert F, Kaneko Y, Raimondi S, and Rabitts TH. Multiple methylation-free islands flask a small breakpoint cluster region on 11p13 in the t(11;14)(p13;q11) translocation. Genes Chromosomes Cancer 1990; **1**: 301–309.
27. Hill RE, Favor J, Hogan BLM, Tom CC, Saunders GF, Handon IM, Prosser J, Jordan T, Hastie ND, and Van Heyningen V. Mouse small eye results from mutations in a paired-like homeobox-containing gene. Nature 1991; **354**: 522–525.
28. Moser AR, Pitot HC, and Dove WF. A dominant mutation that predisposes to multiple intestinal neoplasia in the mouse. Science 1990; **247**: 322–324.
29. Edelmann W, Yang K, Kuraguchi M, Heyer J, Lia M, Kneitz B, Fan K, Brown AM, Lipkin M, and Kucherlapati R. Tumorigenesis in *Mlh1* and *Mlh1/Apc1638N* mutant mice. Cancer Res 1999; **59**: 1301–1307.
30. Halberg RB, Katzung DS, Hoff PD, Moser AR, Cole CE, Lubet RA, Donehower LA, Jacoby RF, and Dove WF. Tumorigenesis in the multiple intestinal neoplasia mouse: redundancy of negative regulators and specificity of modifiers. Proc Natl Acad Sci USA 2000; **97**: 3461–3466.
31. Silverman KA, Koratkar R, Siracusa LD, and Buchberg AM. Identification of the Modifier of *Min 2 (Mon2)* locus, a new mutation that influences *Apc*-induced intestinal neoplasia. Genome Res 2002; **12**: 88–97.
32. Song SY, Gannon M, Washington MK, Scoggins CR, Meszoely IM, Goldenring JR, Marino CR, Sandgren EP, Coffey RJ Jr, Wright CV, and Leach SD. Expansion of *Pdx*1-expressing pancreatic epithelium and islet neogenesis in transgenic mice overexpressing transforming growth factor alpha. Gastroenterology 1999; **117**: 1416–1426.
33. Dudley ME, Sundberg JP, and Roopenian DC. Frequency and histological appearance of adenomas in multiple intestinal neoplasia mice are unaffected by severe combined immunodeficiency (scid) mutation. Intl J Cancer 1996; **65**: 249–253.
34. Fazeli A, Steen RG, Dickinson SL, Bautista D, Dietrich WF, Bronson RT, Bresalier RS, Lander ES, Costa J, and Weinberg RA. Effects of *p53* mutations on apoptosis in mouse intestinal and human colonic adenomas. Proc Natl Acad Sci USA 1997; **94**: 10199–10204.
35. Goss KH, Risinger MA, Kordich JJ, Sanz MM, Straughen JE, Slovek LE, Capobianco AJ, German J, Boivin GP, and Groden J. Enhanced tumor formation in mice heterozygous for *Blm* mutation. Science 2002; **297**: 2051–2053.
36. Harada N, Tamai Y, Ishikawa T, Sauer B, Takaku K, Oshima M, and Taketo MM. Intestinal polyposis in mice with a dominant stable mutation of the beta-catenin gene. EMBO J 1999; **18**: 5931–5942.
37. Franklin DS, Godfrey VL, O'Brien DA, Deng C, and Xiong Y. Functional collaboration between different cyclin-dependent kinase inhibitors suppresses tumor growth with distinct tissue specificity. Mol Cell Biol 2000; **20**: 6147–6158.
38. Di Cristofano A, De Acetis M, Koff A, Cordon-Cardo C, and Pandolfi PP. *Pten* and *p27KIP1* cooperate in prostate cancer tumor suppression in the mouse. Nat Genet 2001; **27**: 222–224.
39. Anderson P, McGuire J, Rubio C, Gradin K, Whitelaw ML, Pettersson S, Hanberg A, and Poellinger L. A constitutively active dioxin/aryl hydrocarbon receptor induces stomach tumors. Proc Natl Acad Sci USA 2002; **99**: 9990–9995.
40. Chawengsaksophak K, James R, Hammond VE, Kontgen F, and Beck F. Homeosis and intestinal tumours in *Cdx2* mutant mice. Nature 1997; **386**: 84–87.
41. Takaku K, Miyoshi H, Matsunaga A, Oshima M, Sasaki N, and Taketo MM. Gastric and duodenal polyps in *Smad4 (Dpc4)* knockout mice. Cancer Res 1999; **59**: 6113–6117.
42. Boivin GP, Washington K, Yang K, Ward JM, Pretlow TP, Russell R, Besselsen DG, Godfrey VL, Doetschman T, Dove WF, Pitot HC, Halberg RB, Itzkowitz SH, Groden J, and Coffey RJ. Pathology of mouse models of intestinal cancer: consensus report and Recommendations. Gastroenterology 2003; **214**: 762–777.
43. Velcich A, Yang W, Heyer J, Fragale A, Nicholas C, Viani S, Kucherlapati R, Lipkin M, Yang K, and Augenlicht L. Colorectal cancer in mice genetically deficient in the mucin *Muc2*. Science 2002; **295**: 1726–1729.
44. Li Q L, Ito K, Sakakura C, Fukamachi H, Inoue K, Chi XZ, Lee KY, Nomura S, Lee CW, Han SB, Kim HM, Kim WJ, Yamamoto H, Yamashita N, Yano T, Ikeda T, Itohara S, Inazawa J, Abe T, Hagiwara A, Yamagishi H, Ooe A, Kaneda A, Sugimura T, Ushijima T, Bae SC, and Ito Y. Causal relationship between the loss of *RUNX3* expression and gastric cancer. Cell 2002; **109**: 113–124.
45. Macleod K. Tumor suppressor genes. Cur Opin Genet Develop 2000; **10**: 81–93.
46. Silberg DG, Furth EE, Taylor JK, Schuck T, Chiou T, and Traber PG. *CDX1* protein expression in normal, metaplastic, and neoplastic human alimentary tract epithelium. Gastroenterology 1997; **113**: 478–486.

249 BOVINE GRANULOSA CELLS mRNA EXPRESSION OF PEROXISOME PROLIFERATOR-ACTIVATED RECEPTOR-α AND THE PROTO-ONCOGENE c-Fos

A. Rodriguez[A], *L.J. Royo*[A], *F. Goyache*[A], *C. Diez*[A], *E. Moran*[A], *A. Salas*[B], *and E. Gomez*[A]

[A]Genetica y Reproduccion-SERIDA, Gijon, Spain; [B]Citometria e Inmunotecnologia, Universidad de Oviedo, Oviedo, Spain. email: airodriguez@serida.org

PPARα and c-Fos are involved in regulation of gene expression and are known to be dependent on retinoic acid (RA), which in turn influences oocyte growth and developmental competence (Duque *et al.*, 2002 Hum. Reprod. 17, 2706–2714; Hidalgo *et al.*, 2003. Reproduction 125, 409–416), probably acting in part through granulosa cells. Peroxisome proliferator-activated receptor-α (PPARα) heterodimerizes with the retinoid receptor X (RXR), while c-Jun/c-Fos heterodimerizes with liganded retinoic acid receptors (RARs), then preventing formation of transcription factor activator protein 1 (AP-1) complexes capable of DNA binding. Cellular retinoic acid binding protein (CRABP) limits RA excess and regulates the transcriptional potential of RA; CRABPII has been detected in rat granulosa cells from mature follicles and luteal cells. The aim of this study was to investigate PPARα, c-Fos and CRABPII mRNA expression in bovine granulosa cells. In parallel, other genes whose expression can be influenced by RA were analyzed: luteinizing hormone receptor (LHr), follicle stimulating hormone receptor (FSHr), aromatase and growth hormone (GH). Ovaries were collected at a local abattoir and kept in saline at 30–35°C. Granulosa cells were obtained by aspirating 2- to 7-mm antral follicle contents, pelleted at 700g for 4 min and resuspended in RNA-later (Ambion®). Total RNA was isolated with a NucleoSpin® RNAII kit (Macherey-Nagel), and mRNA was reverse transcribed into single-stranded cDNA using a 1st Strand cDNA Synthesis Kit for RT-PCR (AMV) (Roche). A PCR standard method was made using 1 μL of the cDNA as a template. All PCR primer couples were designed on the basis of the bovine sequence, but c-Fos and CRABPII primers were designed based on the human-murine sequences. Primers within the couple were located in different exons to distinguish DNA from RNA amplification. CRABPII was further investigated in bovine whole ovary, corpus luteum (CL) and liver, in a search for positive controls. Bovine β-actin, 18S and 28S were examined in each sample as positive controls for RNA isolation and cDNA synthesis efficiency. Ten μL of product were loaded into an agarose 2% gel in TBE buffer containing ethidium bromide, and were separated by horizontal electrophoresis. Gels were visualized with ultraviolet light and photographed using a digital camera. Gene expression in granulosa was demonstrated for PPARα, c-Fos, LHr, FSHr, aromatase, GH and controls (β-actin, 18S and 28S) but CRABPII gene did not express in granulosa cells, whole ovary, CL or liver under our experimental conditions. While lacking CRABPII expression remains intriguing, the expressed genes support a role of retinoid pathway within granulosa cells under both in vivo and in vitro conditions, because granulosa cells used in the present experiments were derived from follicles providing oocytes for IVM-IVF. Grant support: Spanish Ministry of Science and Technology (AGL-2002-01175).

250 SPECIFIC GENE KNOCK DOWN OF OCT-4 IN MOUSE PREIMPLANTATION EMBRYOS USING SHORT INTERFERENCE RNA

M.R. Shin[A], *X.S. Cui*[A], *K.A. Lee*[B], *J.H. Jun*[C], *and N.-H. Kim*[A]

[A]Department of Animal Science, Chungbuk National University, Cheongju, Korea; [B]Graduate School of Life Science and Biotechnology, Pochon CHA University, Pochon, Korea; [C]SamSung Cheil Hospital & Woman's Healthcare Center, Seoul, Korea. email: nhkim@chungbuk.ac.kr

RNA interference is used to specifically and effectively inhibit the expression of cognate genes. In the present study we investigated the inhibitory effect of gene expression in mouse embryos developing in vitro by injecting short interference RNA (siRNA). Fertilized mouse zygotes were obtained from mated females 20–24 h after hCG injection. Chemically synthesized 21-nt siRNA was commercially obtained and injected into mouse zygotes. The zygotes were then cultured in KSOM medium supplemented with 4% BSA at 37°C. Semi-quantitative RT-PCR was used to examine Octamer-binding transcription factor (Oct-4) gene expression in a single mouse embryo developing in vitro following siRNA-injection. In order to determine the expression and distribution of Oct-4 in mouse embryos, the mouse embryos were fixed in 4% paraformaldehyde for 20 min and permeabilized with 0.2% triton x-100 for 10 min. Embryos were then incubated with rabbit Oct-4 polyclonal antibody for 1 h and with FITC-labeled goat anti-rabbit antibody. Propidium iodide was used for DNA staining. siRNA injection did not retard the development of mouse zygotes. The number of blastocyst cells and the ICM/TE ratio did not differ in the siRNA injected blastocysts and the non-injected control group. Semi-quantitative RT-PCR revealed that Oct-4 expression was decreased at the 4-cell embryo stage and was significantly high at the morula and blastocyst stages. Injection of siRNA into oocytes inhibited RNA expression of Oct-4 and Nanog, but not of E-cadherin and Heat shock protein 70.1: Immunocytochemical staining showed inhibition of Oct-4 synthesis of the morulae and blastocysts following injection of siRNA. After culture of the embryos in the ES cell-derived conditioned medium, the embryos were stained for alkaline phosphatase (AP), a marker specific to pluripotent cells. AP was not detected in the inner cell mass of blastocysts following siRNA injection. These results suggest that siRNA injection into a mouse zygote specifically inactivates Oct-4 in mouse embryos developing in vitro.

251 SEARCH FOR GENES INVOLVED IN DEVELOPMENTAL COMPETENCE IN MOUSE OOCYTES USING SUPPRESSION SUBTRACTIVE HYBRIDIZATION

O. Suzuki, T. Hata, M. Koura, Y. Noguchi, K. Takano, Y. Yamamoto, and J. Matsuda

National Institute of Infectious Diseases, Tokyo, Japan. email: osuzuki@nih.go.jp

During the first month after birth, synchronous follicular growth occurs in the ovary of immature mice (first wave). Previously, we showed that mouse oocytes during the first wave were more competent developmentally in older females (Suzuki O *et al.*, 2002 Theriogenology 57, 628 abst), although the numbers of mature oocytes did not differ with female age (17, 18, and 24 days old). In this study, we examined the genetic factors that affect the developmental competence of mouse oocytes during the first wave using suppression subtractive hybridization (SSH). Oocytes collected from 17- and 24-day-old B6D2F1 females (D17 and D24, respectively) without hormonal treatment were matured in Waymouth medium supplemented

with pyruvate (0.23 mM), antibiotics, bovine fetuin (1 mg mL^{-1}), and polyvinylpyrrolidone (3 mg mL^{-1}). After 17-h culture at 37°C in an atmosphere of 5% CO_2, 5% O_2, and 90% N_2, total RNA was isolated from oocytes whose germinal vesicles had broken down (mature oocytes), separately, in three independent culture groups per age (each group contained oocytes from four animals) using Cell-to-cDNA Cell Lysis Buffer (Ambion, Austin, TX, USA). Some of the total RNA from each independent group was pooled by age (total of RNA from approximately 100 oocytes per age) and used for SSH. A SMART cDNA Synthesis Kit (Clontech, Palo Alto, CA, USA) was used to reverse-transcribe total RNA to cDNA. SSH was performed with a PCR-Select cDNA Subtraction Kit (Clontech). The subtracted PCR products were cloned into pGEM-T vector (Promega, Madison, WI, USA). Clones from the subtracted library (D24−D17) were sequenced and their identities were examined using the NCBI BLAST search. The differential expression of candidate genes preferentially expressed in mature D24 oocytes suggested by SSH was confirmed with cDNA transcribed separately in the three independent culture groups per age using real-time quantitative PCR with an ABI Prism 7900HT with TaqMan technology (Applied Biosystems, Foster City, CA, USA). Of 513 clones sequenced, the top six preferentially-expressed candidate genes in more developmentally-competent D24 oocytes were spindlin (20 clones), bmi-1 (4 clones), cyclin B1 (4 clones), E330034G19Rik (4 clones), Jagged1 (4 clones), and Ndfip2 (4 clones). The expression of spindlin in mature D24 oocytes (relative threshold cycle: -3.8 ± 0.7, mean ± SD) was confirmed to be approximately 11-fold higher than in D17 oocytes (-0.3 ± 1.5) when GAPDH was used as an internal control ($P < 0.05$, *t*-test). Quantitative analyses of mRNA expression of the remaining genes are now under way. Our results suggest that spindlin is one of the key factors leading to the acquisition of developmental competence in mouse oocytes during folliculogenesis. Supported by JSPS KAKENHI (No.145716000) and MHLW.

252 A COMPARATIVE EXPRESSION ANALYSIS OF GENES IN PREIMPLANTATION DEVELOPMENTAL STAGES OF BOVINE EMBRYOS PRODUCED IN VITRO OR IN VIVO

D. Tesfaye, K. Wimmers, M. Gilles, S. Ponsuksili, and K. Schellander

Institute of Animal Breeding Science, Bonn, Germany. email: tesfaye@itz.uni-bonn.de

A comparative analysis of mRNA expression patterns between embryos produced under different in vitro and in vivo culture systems allows the isolation of genes associated with embryo quality and investigation of the effect of culture environment on the embryonic gene expression. In this study, expression analysis of four known (PSCD2, TCF7L2, NADH-subunit and PAIP1) genes and one novel transcript, derived from differential display PCR, was performed in in vitro (Ponsuksili *et al.*, 2002, Theriogenology 57, 1611–1624) or in vivo- (Moesslacher *et al.*, 2001 Reprod. Dom. Anim. 32, 37) produced bovine 2-, 4-, 8-, 16-cell, morula and blastocyst stage embryos using real time PCR technology. Poly(A) RNA was isolated from four separate individual embryos from each developmental stage and embryo group (in vitro or in vivo) using Dynabeads mRNA kit (Dynal, Oslo, Norway). After reverse transcription, quantitative PCR was performed with sequence specific primers in an ABI PRISM® 7000 Sequence Detection System instrument (Applied Biosystems, Foster City, CA, USA) using SYBR® Green as a double-strand DNA-specific fluorescent dye. Standard curves were generated for target and endogenous genes using serial dilutions of plasmid DNA. Final quantification was done using the relative standard curve method, and results were reported as relative expression or *n*-fold difference to the calibrator cDNA (i.e., the blastocyst stage) after normalization with the endogenous control (Histone2a). Data were analyzed using SAS version 8.0 (SAS Institute Inc., NC, USA) software package. Analysis of variance was performed with the main effects being the developmental stage and embryo source (in vitro or in vivo) and their interactions followed by multiple pairwise comparisons using Tukey's test. No significant difference was observed in the relative abundance of the PSCD2 gene between the two embryo groups. However, its expression was higher (20-fold) ($P < 0.05$) at the 8-cell stage than the other developmental stages among in vitro embryos. Higher expression ($P < 0.05$) of NADH-subunit mRNA was detected in vivo than in vitro at the 2-cell stage of development. The TCF7L2 mRNA was expressed in the in vitro embryos but not in the in vivo ones. PAIP1 mRNA was higher ($P < 0.05$) in in vitro (1500-fold) than in the in vivo embryos (500-fold) at the 2-cell developmental stage compared to the calibrator. The novel transcript was also detected at higher level ($P < 0.05$) in the in vitro than in the in vivo embryos at the 2-cell stage of development. However, the PAIP1 and the novel transcript showed no significant difference in their expression between the two embryo groups beyond the 2-cell developmental stage. Both PAIP1 and the novel transcript were detected only up to 8-cell stage in both embryo groups, suggesting their maternal origin. In conclusion, the variations in the expression of studied genes between in vitro and in vivo may reflect the effect of the two culture systems on the transcriptional activity of early embryos.

253 BOVINE OOCYTE CYCLIN B1 mRNA UNDERGOES CYTOPLASMIC POLYADENYLATION BEFORE THE BEGINNING OF IN VITRO MATURATION

K. Tremblay, C. Vigneault, G. Bujold, and M.-A. Sirard

Laval University, Quebec City, Quebec, Canada. email: karinetremblaycrbr@hotmail.com

Maternal oocyte Cyclin B1 mRNA is known to be stored in the cytoplasm with a short poly(A) tail and be translationally dormant at GV stage. During maturation, Cyclin B1 poly(A) tail is elongated by a process called cytoplasmic polyadenylation and driven by A/U-rich cis-acting elements in its 3′ untranslated region (UTR) known as cytoplasmic polyadenylation elements (CPEs). The objective of this study was to elucidate whether GV-stage bovine oocytes possess a stockpile of Cyclin B1 mRNA stored with a short a poly(A) tail that is elongated during maturation by CPE regulation. The mRNA poly(A) tail length was measured by Rapid Amplification of cDNA Ends Polyadenylation test (Race-PAT) on oocytes ($n = 100$) at the GV stage and 3, 5, 8, 10, 15, 20, and 25 h of in vitro maturation. The mRNA poly(A) tail length was also measured in triplicate ($n = 20$) on cold oocytes in GV (all manipulations on ice), warm oocytes in GV (ovaries transported in warm saline and manipulations on ice) and warm + 2 h 30 min oocytes in GV (oocytes left for an additional 2 h and 30 min at room temperature). To assess for variation in mRNA quantity, Cyclin B1 mRNA level was quantified by real-time PCR (Lightcycler, Roche, Indianapolis, IN, USA) in cold, warm or warm + 2 h

Do cloned mammals skip a reprogramming step?

Josef Fulka Jr., Norikazu Miyashita, Takashi Nagai & Atsuo Ogura

It is widely accepted that at least some populations of cloned animals have an attenuated lifespan compared with their conventionally bred counterparts. This has been attributed both to premature aging or senescence and to accumulation of abnormalities in gene expression in their tissues. Here, we argue that these problems arise because the process of nuclear transfer used to create cloned animals skips one of the two essential, independent steps involved in the reprogramming of cell nuclei.

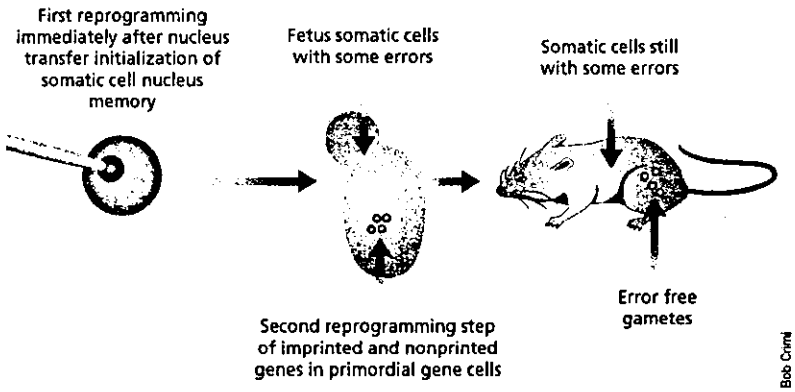

Figure 1 Reprogramming in two steps. The first step occurs after the nucleus is transferred into the enucleated oocyte and probably during the next few divisions, depending on the species. In about 1–5% of reconstructed oocytes, this reprogramming, even with some errors, permits further development and results in viable offspring. In the remaining cases, the reprogramming is incomplete and embryos die or offspring are not viable. During the second reprogramming step, imprinted and nonimprinted genes are reprogrammed, and errors that were not corrected during the first step are repaired. As this step occurs only in the germline cells, cloned animals contain somatic cells with some abnormalities, but their spermatozoa or oocytes are error-free.

Senescence

Since the birth of Dolly the sheep in 1996, the 'real biological age' of cloned animals has been a matter of much debate[1]. It has been argued that Dolly was either 6 years old (on the basis of her date of birth) or 12 years old (on the basis of the age of the donor mammary gland cell used in her creation) when she was euthanased because of serious progressive lung disease.

One proposed means of assessing a clone's age is by measuring the length of its telomeres and the speed of their erosion. Simple measurements of telomere length suggest that cloned animals have telomeres that are similar in length to, or even longer than, telomeres from naturally bred animals[2–5]. Telomeres from Dolly[6] and from bovine clones[7] are shorter than those of age-matched controls, however. In addition, certain cloned animals have even shorter telomeres than those in the somatic donor cells from which they were actually derived. As many cloned large animals reach 4–6 years of age with no signs of premature aging, these variations and errors in telomere restoration do not necessarily seem to lead to premature aging.

A comparison by Clark *et al.*[8] of *in vitro* culture parameters and characteristics of sheep fibroblast cells used as nuclear donors in cloning and cells derived from corresponding cloned fetuses showed that complete telomere restoration is not necessarily achieved after nuclear transfer; in fact, the proliferation and lifespan of the cloned cells from the fetus are the same as those of the donor cell line. The authors thus concluded that the lifespan of a clone is influenced by the genetically determined speed of telomere erosion.

Because of their short life cycle, mice are an ideal system for studying the longevity of cloned animals. A study by Ogonuki *et al.*[9] showed that cloned mice die significantly earlier than controls. As many of the cloned mice suffer from serious pathologies (*e.g.*, pneumonia and hepatic failure), however, premature aging might not be the primary cause of death.

What is normal?

This raises the question of whether any clones are completely 'normal'[10]? The expression of several (imprinted and nonimprinted) genes differs substantially in cloned animals compared with conventionally bred counterparts. Of about 10,000 genes analyzed in mouse clones, approximately 400 show abnormal expression patterns, especially in placentas[11]. Notably, aberrant expression seems to be somewhat tissue-specific, with nonplacental organs having a lesser extent of abnormal gene expression.

A similar analysis of expression of genes in the *Oct4* group in mice showed that embryos derived from embryonic stem cells have a normal expression pattern[12,13], whereas blastocysts produced by somatic cell transfer have abnormal expression (additional factors, *e.g.*, culture conditions, may also influence the expression of certain genes[14,15]). Thus, we conclude that the premature aging of clones is not the only (or the main) reason why cloned animals die earlier than naturally bred counterparts.

Reprogramming by steps

To elucidate this phenomenon, we must look more closely at the reprogramming of the nucleus after its transfer to the recipient cell. There are essentially two independent natural periods when cell nuclei can be reprogrammed. The first period begins immediately after fertilization when, for example, the

J.F. Jr. is in Center for Cell Therapy and Tissue Repair, Prague, DOB1, CS-104 01, Prague 10, Czech Republic; N.M. and T.N. are in the National Institute of Agrobiological Sciences, Tsukuba, Kannondai 2-1-2, 305-8602 Japan; and A.O. is in RIKEN BioResource Center, 3-1-1, Koyadai, ScubaInstitute, Tsukuba, 305-0074, Japan. e-mail: taku@affrc.go.jp

paternal chromatin is intensively demethylated. The embryo methylation level reaches its lowest phase at the blastocyst stage (by day 3.5 in the mouse), and the methylation pattern is gradually established thereafter, the exact time depending on the cell line[16,17].

The second reprogramming period occurs in developing germline cells. For example, in mouse primordial germ cells, the imprinting memory established in parental gametes is erased between days 10 and 12 of pregnancy[18]. On the basis of cloning studies, we may assume that the purpose of this second reprogramming phase is to erase, by as yet unknown mechanisms, all the epigenetic errors that had been accumulated before, and that this reprogramming step enhances the chance of producing error-free gametes.

Thus, at fertilization, both spermatozoa and oocytes should be epigenetically error-free. Certainly, this is not the case for a somatic cell nucleus used for nuclear transfer. Moreover, fertilization has been honed by millions of years of evolution to ensure that sperm (donor) and oocyte (recipient) are uniquely prepared to ensure fidelity of nuclear imprinting.

We suggest that, at present, a complete reprogramming in cloning is only possible through these two steps (Fig.1). The first reprogramming step occurs in oocytes to initialize the memory of the differentiated somatic cells. The second reprogramming step occurs as chosen cells (primordial germ cells and their successor cells) in a given clone pass through the germ-cell formation processes. This is also supported by results from obese or otherwise abnormal mouse clones, whose phenotypes are not manifested in their offspring[19,20]. Also, telomeres in spermatozoa from cloned bulls are the same length as telomeres in controls, whereas telomeres in their somatic cells are shorter[7,21]. This supports the notion that gametes in clones are error-free[19,20]. There is, however, no chance of developing cloned animals whose cells pass through the second step[22].

Conclusions

During reproduction, reprogramming occurs in two steps. The first reprogramming event results in the initial de-differentiation of the transferred nucleus, making it competent to direct the development of the embryo. The second reprogramming event has at least three roles: first, epigenetic errors are erased (by as yet unknown mechanisms); second, genomic imprinting is erased and reestablished; and third, telomere length is adjusted definitively, following elongation at the first reprogramming and subsequent gametogenesis.

We presume that cloned animals die earlier not because they are biologically too old, but because they accumulate abnormalities in expression of different genes. When single cells are isolated from cloned fetuses or animals, their proliferation and viability are normal[8]. This has also been recently shown in intestine-derived cloned blastulae from amphibians that were transferred to normal host embryos; after several months, the transferred cells contributed to several host tissues[23].

Our conclusions have several implications for biotechnology. First, cells obtained by 'therapeutic cloning' will probably have the same life span as normal cells but may have abnormal gene expression caused by epigenetic errors. Second, the progeny of cloned animals will be normal. This is especially important for the use of cloned animals in xenotransplantation or the production of valuable pharmaceutical proteins in their milk[24,25]. Third, and perhaps most important, the problems stated above argue against the application of human reproductive cloning. The incomplete reprogramming of donor nuclei during somatic cell nuclear transfer will probably have such dire effects on gene expression and health that the production of children by such techniques as presently available should be prohibited.

ACKNOWLEDGMENTS

J.F.Jr. appreciates support from The Japan Society for the Promotion of Sciences (S03152).

1. Wilmut, I., Schnieke, A.E., McWhir, J., Kind, A. & Campbell, K.H.S. *Nature* **385**, 810–813 (1997).
2. Lanza, R.P. *et al. Science* **288**, 665–669 (2000).
3. Tian, X.C., Xu, J. & Yang, X. *Nat. Genet.* **26**, 272–273 (2000).
4. Wakayama, T. *et al. Nature* **407**, 318–319 (2000).
5. Betts, D.H. et al. Proc. Natl. Acad. Sci. USA **96**, 1077–1082 (2001).
6. Shiels, P.G. *et al. Nature* **399**, 316–317 (1999).
7. Miyashita, N. *et al. Biol. Reprod.* **66**, 1649–1655 (2002).
8. Clark, A.J. *et al. Nat. Cell Biol.* **5**, 535–538 (2003).
9. Ogonuki, N. *et al. Nat. Genet.* **30**, 253–254 (2002).
10. Wilmut, I. *Nat. Med.* **8**, 215–216 (2002).
11. Humpherys, D. *et al. Proc. Natl. Acad. Sci. USA* **99**, 12889–12894 (2002).
12. Boiani, M., Eckardt, S., Scholer, H.R. & McLaughlin, K.J. *Genes Dev.* **16**, 1209–1219 (2002).
13. Bortvin, A. *et al. Development* **130**, 1673–1680 (2003).
14. Rideout III, W.M., Eggan, K. & Jaenisch, R. *Science* **293**, 1093–1098 (2001).
15. Wilmut, I. *et al. Nature* **419**, 583–586 (2002).
16. Reik, W. & Walter, J. *Nat. Rev. Genet.* **2**, 21–32 (2001).
17. Li, E. *Nat. Rev. Genet.* **3**, 662–673 (2002).
18. Lee, J. *et al. Development* **129**, 1807–1817 (2002).
19. Tamashiro, K.L.K. *et al. Nat. Med.* **8**, 262–267 (2002).
20. Shimozawa, N. *et al. Genesis* **34**, 203–207 (2002).
21. Miyashita, N. *et al. Theriogenology* **59**, 1557–1565 (2003).
22. Hochedlinger, K. & Jaenisch, R. *N. Engl. J. Med.* **349**, 275–286 (2003).
23. Byrne, J.A., Simonsson, S. & Gurdon, J.B. *Proc. Natl. Acad. Sci. USA* **99**, 6059–6063 (2002).
24. Prather, R.S., Hawley, R.J., Carter, D.B., Lai, L. & Greenstein, J.L. *Theriogenology* **59**, 115–123 (2003).
25. Robl, J.M. *et al. Theriogenology* **59**, 107–113 (2003).

genesis 39:79-83 (2004)

LETTER

Tissue-Specific Distribution of Donor Mitochondrial DNA in Cloned Mice Produced by Somatic Cell Nuclear Transfer

Kimiko Inoue,[1] Narumi Ogonuki,[1] Yoshie Yamamoto,[2] Kaoru Takano,[2] Hiromi Miki,[3] Keiji Mochida,[1] and Atsuo Ogura[1]*

[1]RIKEN Bioresource Center, Tsukuba, Ibaraki, Japan
[2]Department of Veterinary Science, National Institute of Infectious Diseases, Shinjuku, Tokyo, Japan
[3]Meiji University, Kawasaki, Kanagawa, Japan

Received 13 November 2003; Accepted 28 January 2004

Summary: Highly diverse results have been reported for mitochondrial DNA (mtDNA) hetero-plasmy in nuclear-transferred farm animals. In this study, we cloned genetically defined mice and investigated donor mtDNA inheritance following somatic cell cloning. Polymerase chain reaction (PCR) analysis with primers that were specific for either the recipient oocytes or donor cells revealed that the donor mtDNA coexisted with the recipient mtDNA in the brain, liver, kidney, and tail tissues of 96% (24/25) of the adult clones. When the proportion of donor mtDNA in each tissue was measured by allele-specific quantitative PCR and subjected to ANOVA analysis, a tissue-specific mtDNA segregation pattern ($P < 0.05$) was observed, with the liver containing the highest proportion of donor mtDNA. Therefore, the donor mtDNA was inherited consistently by the cloned offspring, whereas donor mtDNA segregation was not neutral, which is in accordance with previous notions about tissue-specific nuclear control of mtDNA segregation. genesis 39:79–83, 2004. © 2004 Wiley-Liss, Inc.

Key words: mitochondrial DNA; cloning; mouse; embryo; somatic cell

The production of animals by somatic cell cloning is now possible in several mammalian species, including sheep, mice, cattle, goats, pigs, cats, rabbits, mules, and horses (Wilmut *et al.*, 2002; Galli *et al.*, 2003; Woods *et al.*, 2003). The derived clones are considered genetic duplicates of the donor nuclear genome that was used for the nuclear transfer. However, since the recipient oocytes contain 10^2 to 10^3 times higher copy numbers of mtDNA, as compared to the donor cells, the resultant cloned animals are assumed to be transmitochondrial, i.e., having nuclear and mitochondrial genomes of different origins. Evans *et al.* (1999) analyzed mtDNA inheritance in Dolly the sheep, derived from an adult somatic cell line, and in nine sheep that were derived from fetal cells, and found that the mtDNAs in these clones were exclusively oocytic in origin. This result indicates that the donor mtDNA is eliminated by unknown mechanisms after nuclear transfer, and that only the mtDNA from oocytes proliferates in cloned animals. However, contrasting results were obtained when more sensitive polymerase chain reaction (PCR) methods were employed for the detection of mtDNA. Steinborn *et al.* (2000) revealed that the donor mtDNA could be detected in seven out of ten somatically cloned cattle produced by electrofusion, with the donor mtDNA comprising 0.4–4% of the total number of mtDNA copies, which indicates that mtDNA heteroplasmy occurs in the majority of cloned animals. They estimated that the ratio of donor cells to recipient cytoplast mtDNAs before nuclear transfer was in the range of 0.4–0.8%. Thus, it appears that the levels of donor mtDNAs are maintained throughout clone development, whereas they may increase or decrease at certain times during development. However, more recent analyses by other researchers using bovines have added further layers of complexity to this topic by describing a variety of potential donor mtDNA fates, e.g., neutral segregation (Steinborn *et al.*, 2002; Hiendleder *et al.*, 2003), significant reductions (Meirelles *et al.*, 2001), and significant increases (Takeda *et al.*, 2003). These discrepancies may be due, at least in part, to the preexisting heteroplasmy in recipient oocytes (Takeda *et al.*, 2003), the types of donor cell used, and the tissues examined.

Since the initial success of mouse somatic cell cloning in 1998 (Wakayama *et al.*, 1998), this experimental system has provided valuable information on the phenotypes and gene expression profiles that are specific to cloned embryos/animals (Ogura *et al.*, 2001). The biological advantages of laboratory mice over domestic species, which include the availability of well-characterized

* Correspondence to: Atsuo Ogura, D.V.M., Ph.D., RIKEN Bioresource Center, 3-1-1, Koyadai, Tsukuba, Ibaraki 305-0074, Japan.
E-mail: ogura@rtc.riken.go.jp
Contract grant sponsors: MEXT (Japan), MHLW (Japan), CREST (Japan), and the Human Science Foundation (Japan).
Published online in
Wiley InterScience (www.interscience.wiley.com)
DOI: 10.1002/gene.20029

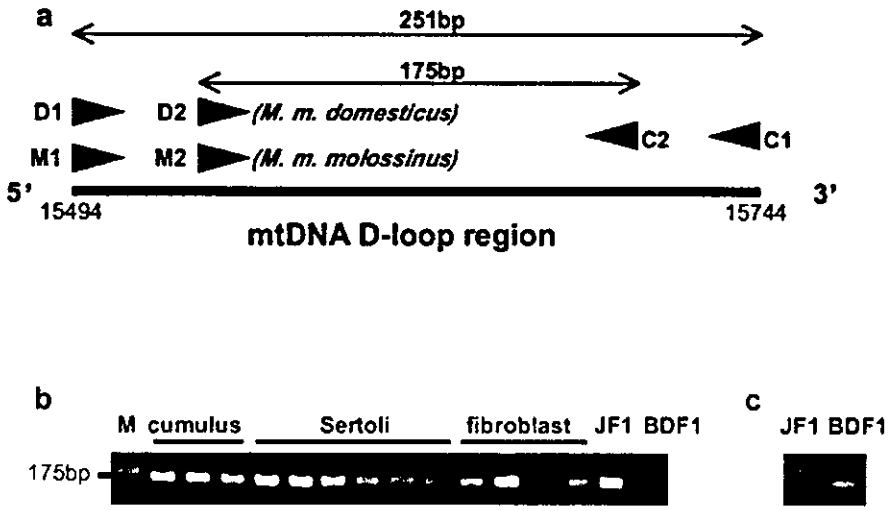

FIG. 1. a: Localization of the primers from the mouse D-loop region used for qualitative and quantitative analyses of mtDNA and the corresponding PCR product sizes. These primers were slightly modified from those reported previously (Kaneda *et al.*, 1995). The origin of the mtDNA was identified as the oocyte (B6D2F1) by the primer set D2 and C2, and as the donor (JF1) by the primer set M2 and C2. **b,c:** Detection of JF1 and B6D2F1 mtDNAs in the brains of cloned mice (cumulus, Sertoli, and fibroblast cells) and control mice (JF1 and BDF1). Amplification was carried out using the primer sets indicated in **a**. Donor (JF1) mtDNA was detected by a combination of M2 and C2 (**b**). B6D2F1 mtDNA was detected by a combination of D2 and C2 (**c**). Each primer set amplified specifically one type of mtDNA, as shown for the control samples (JF1 and B6D2F1).

genotypes, short pregnancy period, and rapid generational turnover, enable large-scale systematic analyses of the genetic, biochemical, and pathological characteristics of cloned animals (reviewed in Ogura *et al.*, 2002). The present study was undertaken to investigate the fate of the donor mtDNA in mice that were cloned from different cell types from a single genetic background.

The donor nuclei were transferred into enucleated oocytes by direct injection (for cumulus cells and Sertoli cells) or electrofusion (for fibroblast cells). The mouse strain that was used as the nuclear donor was (JF1 × 129/Sv-*ter*)F1, which was generated by crossing JF1 (*Mus musculus molossinus*) females and 129/Sv-*ter* (*M. m. domesticus*) males in our laboratory. Due to the exclusive maternal inheritance of mitochondria, the nuclear donor mice had JF1-origin mitochondria. Since the recipient B6D2F1 (C57BL/6 × DBA/2) oocytes had C57BL/6 (*M. m. domesticus*) mitochondria, the mtDNAs of different origin were distinguishable in the tissues of the cloned mice, based on mtDNA sequence polymorphisms between the subspecies.

After the transfer of 472 embryos into recipient uteri, we obtained 29 cloned fetuses at term. Three of the clones were from cumulus cells, 19 from immature Sertoli cells, and seven from tail tip fibroblasts. All of the fetuses were alive when retrieved from the uteri and showed active movement. Of these, three, 16, and six pups, respectively, grew into normal adults. The birth rate (6.1%) and survival rate into adulthood (86.2%) were within the normal range for cloned mice in our laboratory (Inoue *et al.*, 2002, 2003).

Total DNA samples from the brain, liver, kidney, and tail were subjected to allele-specific PCR analysis based on mtDNA polymorphisms. The primer sets (Fig. 1a) specifically amplified mtDNA molecules of different origins, as shown in Figure 1b,c. This polymorphism analysis revealed that 24/25 cloned mice (cumulus: 3/3; Sertoli: 16/16; fibroblasts: 5/6) possessed mtDNA from the donor cells in all of the tissues examined (Fig. 1b). We conclude that donor mtDNA produces mtDNA heteroplasmy in cloned adults.

Oocytes have the ability to recognize sperm-derived mitochondria of the same species and to eliminate paternal mtDNA, probably via a mechanism that involves ubiquitin (Sutovsky *et al.*, 1999, 2000). Since ubiquitination of sperm mitochondrial membrane proteins occurs during spermatogenesis (Chen *et al.*, 1998; Baarends *et al.*, 1999), it seems likely that the mitochondria of the donor somatic cells escape from proteolysis in the egg cytoplasm upon nuclear transfer. During the subsequent preimplantation stage, since the donor mtDNA in the reconstructed embryo has the same origin as the embryonic nuclei, incompatibility does not arise. Thus, it is reasonable to assume that no mechanism exists that actively eliminates donor-derived mtDNAs that are cointroduced with the donor nucleus, which ensures the survival of the bulk of the donor mtDNA in the majority (96%) of our cloned mice.

For quantitative PCR analysis, we first determined the time-lapse amplification patterns using the *M. m. molossinus* mtDNA specific primer set. The correlation coefficients of the six threshold cycle (Ct) plots for the